# 2

# Synthesis and Photophysical Properties of Pyrene-Based Multiply Conjugated Shaped Light-Emitting Architectures: Toward Efficient Organic-Light-Emitting Diodes

Jian-Yong Hu[1,2] and Takehiko Yamato[1]
[1]*Department of Applied Chemistry, Faculty of Science and Engineering, Saga University*
[2]*Department of Organic Device Engineering, Yamagata University*
*Japan*

## 1. Introduction

Since the pioneering works on the first double-layer thin-film Organic electroluminescence (EL) devices (OLEDs) by C. W. Tang and co-workers in the Kodak Company in 1987 (Tang & Vanslyke, 1987), OLEDs have attracted enormous attentions in the scientific community due to their high technological potential toward the next generation of full-color-flat-panel displays (Hung & Chen, 2002; Wu et al., 2005; Geffroy et al., 2006) and lighting applications (Duggal et al., 2007; So et al., 2008). In today's developments of OLED technologies, the trends of organic EL devices are mainly focusing both on optimizations of EL structures and on developing new optoelectronic emitting materials. Obviously the key point of OLEDs development for full-color-flat display is to find out materials emitting pure colors of red, green and blue (RGB) with excellent emission efficiency and high stability. Numerous materials with brightness RGB emission have been designed and developed to meet the requirements toward the full-color displays. Among them, organic small molecules containing polycyclic aromatic hydrocarbons (PAHs) (e. g. naphthalene, anthracene, perylene, fluorene, carbazole, pyrene, etc.) are well known and are suitable for applications in OLEDs. Recently, naphthalene, anthracene, perylene, fluorene, carbazole, pyrene and their derivatives have been widely used as efficient electron-/hole-transporting materials or host emitting materials in OLED applications. In this chapter an overview is presented of the synthesis and photophysical properties of pyrene-based, multiply conjugated shaped, fluorescent light-emitting materials that have been disclosed in recent literatures, in which several pyrenes have been successfully used as efficient hole-/electron-transporting materials or host emitters or emitters in OLEDs, by which a series of pyrene-based, cruciform-shaped π-conjugated blue-light-emitting architectures can be prepared with an emphasis on how synthetic design can contribute to the meeting of promising potential in OLEDs applications.

## 2. Pyrene and pyrene derivatives

Pyrene is an alternant polycyclic aromatic hydrocarbon (PAH) and consists of four fused benzene rings, resulting in a large, flat aromatic system. Pyrene is a colorless or pale yellow

solid, and pyrene forms during incomplete combustion of organic materials and therefore can be isolated from coal tar together with a broad range of related compounds. Pyrene has been the subject of tremendous investigation. In the last four decades, a number of research works have been reported on both the theoretical and experimental investigation of pyrene concerning on its electronic structure, UV-vis absorption and fluorescence emission spectrum. Indeed, this polycyclic aromatic hydrocarbon exhibits a set of many interesting electrochemical and photophysical attributes, which have results in its utilization in a variety of scientific areas. Some recent advanced applications of pyrene include fluorescent labelling of oligonucleotides for DNA assay (Yamana et al., 2002), electrochemically generated luminescence (Daub et al., 1996), carbon nanotube functionallization (Martin et al., 2004), fluorescence chemosensory (Strauss & Daub, 2002; Benniston et al., 2003), design of luminescence liquid crystals (de Halleux et al., 2004), supermolecular self-assembly (Barboiu et al., 2004), etc.. On the other hand, as mentioned above, PAHS (e. g. naphthalene, anthracene, perylene, fluorene, carbazole, etc.) and their derivatives have been developed as RGB emitters in OLEDs because of their promising fluorescent properties (Jiang et al., 2001; Balaganesan et al., 2003; Shibano et al., 2007; Liao et al., 2007; Thomas et al., 2001). In particular, these compounds have a strong π-electron delocalization character and they can be substituted with a range of functional groups, which could be used for OLEDs materials with tuneable wavelength. Similarly, pyrene has strong UV-vis absorption spectra between 310 and 340 nm and emission spectra between 360 and 380 nm (Clar & Schmidt, 1976), especially its expanded π-electron delocalization, high thermal stability, electron accepted nature as well as good performance in solution. From its excellent properties, it seems that pyrene is suitable for developing emitters to OLEDs applications; however, the use of pyrene molecules is limited, because pyrene molecules easily formed π-aggregates/excimers and the formation of π-aggregates/excimers leads to an additional emission band in long wavelength and the quenching of fluorescence, resulting in low solid-state fluorescence quantum yields. Recently, this problem is mainly solved by both the introduction of long or big branched side chains into pyrene molecules and co-polymerization with a suitable bulky co-monomer. Very recently, it was reported that pyrene derivatives are useful in OLEDs applications (Otsubo et al., 2002; Thomas et al., 2005; Ohshita et al., 2003; Jia et al., 2004; Tang et al., 2006; Moorthy et al., 2007) as hole-transporting materials (Thomas et al., 2005; Tang et al., 2006) or host blue-emitting materials (Otsubo et al., 2002; Ohshita et al., 2003; Jia et al., 2004; Moorthy et al., 2007). To date, various pyrene-based light-emitting materials have been disclosed in recent literatures, which can be roughly categorized into three types of materials: (1) *Functionalized pyrene-based light-emitting monomers;* (2) *Functionalized pyrene-based light-emitting dendrimers*; and (3) *Functionalized pyrene-based light-emitting oligomers and polymers.*

## 3. Functionalized pyrene-based light-emitting monomers

Because of its extensive π-electron delocalization and electron-accepted nature, pyrene is a fascinating core for developing fluorescent π-conjugation light-emitting monomers. In those compounds, pyrene was used as a conjugation centre core substituted by some functionalized groups or as function substituents introduced into others PAHs rings. In this section, the synthesis and photophysical properties of two types of functionalized pyrene-based light-emitting monomers, namely, *pyrene-cored organic light-emitting monomers* and *pyrene-functionalized PAHs-cored organic light-emitting monomers* were fully presented. In particular, the use of these light-emitting monomers as efficient emitters in OLEDs will be discussed in detail.

### 3.1 Pyrene-cored organic light-emitting monomers

Although pyrene and its derivatives have been widely used as fluorescence probes in many applications, there are two major drawbacks using pyrene as a fluorescence probe: One is the absorption and emission wavelengths of the pyrene monomer are confined to the UV region of 310-380 nm, and the other is pyrene can easily forms an excimer above concentrations of 0.1 mM. In order to probe biological membranes using fluorescence techniques it is desirable to have a fluorophore probe that absorbs and emits in the long wavelength region, preferably in the visible region of the electromagnetic spectrum in order to minimize the spectral overlap of the intrinsic fluorescence of the bio-molecules that occur in the UV region. Furthermore, molecular systems that are light emitters in the visible region are potentially useful in the fabrication of organic light emitting diodes (OLEDs). Therefore, it is desirable to design molecules that have emission in the visible region. Consequently, the most common method to bathochromically shift the absorption and emission characteristics of a fluorophore is to extend the π-conjugation by introducing unsaturated functional groups (e. g. acetylenic group) or rigid, bulky PAHs moieties (e. g. phenylene, thiophene, bithiophene, thienothiophene, benzothiadiazole-thiophene, pridine, etc.) to the core of the fluorophore. In recent papers, using pyrene as a conjugation centre core, the synthesis, absorption and fluorescence-emission properties of the 1,3,6,8-tetraethynylpyrenes and its derivatives have been reported (Venkataramana & Sankararaman 2005, 2006; Fujimoto et al., 2009), and monomers of 1-mono, 1,6-bis-, 1,8-bis-, 1,3,6-tris-, and 1,3,6,8-tetrakis-(alkynyl)pyrenes have also been prepared (Maeda et al., 2006; Kim et al., 2008; Oh et al., 2009). On the other hand, 1,3,6,8-tetraarylpyrenes as fluorescent liquid-crystalline columns (de Halleux et al., 2004; Sienkowska et al., 2004) or organic semiconductors for organic field effect transistors (OFETs) (Zhang et al., 2006) or efficient host blue emitters (Moorthy et al., 2007; Sonar et al., 2010) or electron transport material (Oh et al., 2009) have recently been reported. The starting point for the above-mentioned synthesis was 1-mono (**2a**), 1,6-di-(**2b**), 1,8-di-(**2c**), 1,3,6-tris-(**2d**), and 1,3,6,8-tetrabromopyrenes (**2e**), which is readily prepared by electrophinic bromination of pyrene (**1**) with one to excess equivalents of bromine under the corresponding reaction conditions, respectively (Grimshaw et al., 1972; Vollmann et al., 1937) (Scheme 1). These materials were consequently converted to the corresponding alkynylpyrenes (pyrene-C≡C-R) or arylpyrenes (pyrene-R) by Sonogashira cross-coupling reaction or Suzuki cross-coupling reaction, respectively.

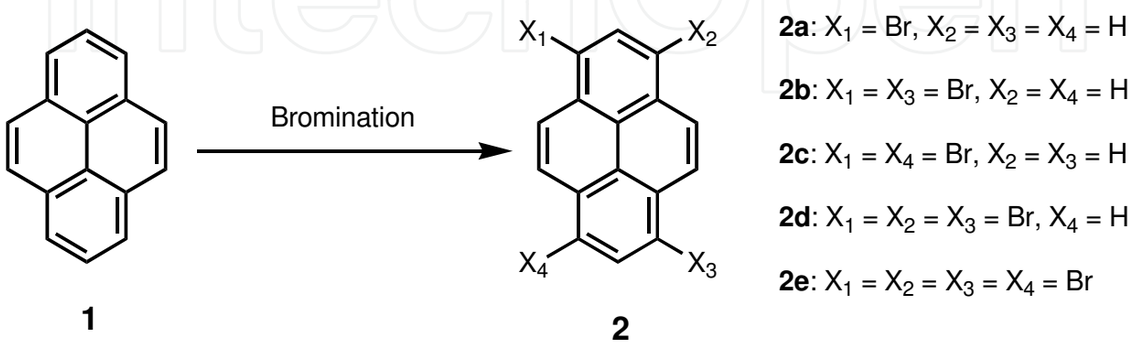


Scheme 1. Electrophilic bromination of pyrene (**1**)

### 3.1.1 Alkynyl-functionalized pyrene-cored light-emitting monomers

Acetylene has been widely applied for linking π-conjugated units and for effectively extending the π-conjugation length. The progress of such π-conjugated materials by means of acetylene chemistry has strongly dependent on the development of Sonogashira coupling reaction. Thereby, many attractive acetylene-linked molecules have emerged such as for semiconducting polymers (Swager et al., 2005; Swager & Zheng, 2005), macrocyclic molecules (Kawase, 2007; Hoger et al., 2005), helical polymers (Yamashita & Maeda, 2008) and energy transfer cassettes (Loudet et al., 2008; Han et al., 2007; Jiao et al., 2006; Bandichhor et al., 2006). Accordingly, the use of acetylene group for extending the conjugation of the pyrene chromophore is one of the most common methods. Sankararaman *et al.* (Venkataramana & Sankararaman, 2005) reported the synthesis, absorption and fluorescence-emission of 1,3,6,8-tetraethynylpyrene derivatives **3a-f**, which were prepared by the Sonogashira coupling of tetrabromomide (**2e**) with various terminal acetylenes yielded the corresponding tetraethynylpyrenes. Significant bathochromic shifts of absorptions band were observed in the region of 350-450 nm for **3a-d**, 375-474 nm for **3e-f**, respectively, compare with that of pyrene (**1**) in dilute THF solutions due to the extended conjugation of the pyrene chromophore with the acetylenic units. Similarly, the fluorescence emission bands of **3a-f** are also bathochromically shifted in region of 420-550 nm in comparison of pyrene in THF. The quantum efficiency of fluorescence emission for **3a-d** was in the rang of 0.4-0.7; these values are comparable to that of pyrene, while **3e** and **3f** are low due to the deactivation of the excited state resulting from the free rotation of the phenyl groups. The results suggest these derivatives are potentially useful as emitters in the fabrication of organic light emitting diodes (OLEDs). A pyrene octaaldehyde derivative **4** and its aggregations through π-π and C-H···O interactions in solution and in the solid state probed by its fluorescence emission and other spectroscopic methods are also prepared by Sankararaman *et al.* (Venkataramana & Sankararaman, 2006) In view of its solid-state fluorescence, this octaaldehyde **4** and its derivatives might find applications in the field of molecular optoelectronics. Similarly, Fujimoto and co-workers (Maeda et al., 2006) have synthesized a variety of alkynylpyrene derivatives **5a-d** from mono- to tetrabromo-pyrenes (**2a-2e**) and arylacetylenes using the Sonogashira coupling, and comprehensively examined their photophysical properties. The alkynylpyrenes **5a-h** thus prepared showed not only long absorption (365-434 nm, 1.0 x $10^{-5}$ M, in EtOH) and fluorescence emission (386-438 nm, 1.6-2.5 x $10^{-7}$ M, in EtOH) wavelengths but also high fluorescence quantum yields (0.55-0.99, standards used were 9,10-diphenylanthracene) as compared with pyrene itself. Additionally, the alkynylpyrene skeletons could be applied to practically useful fluorescence probes for proteins and DNAs. Fujimoto *et al.* (Fujimoto et al., 2009) recently also prepared a series of 1,3,6,8-tetrakis(arylethynyl)pyrenes **6a-e** bearing electron-donating or electron-withdrawing groups. Their photophysical properties analysis demonstrated that the donor-modified tetrakis(arylethynyl)pyrene **6a-c** showed fluorescence solvatochromism on the basis of intramolecular charge transfer (ICT) mechanism, while the acceptor-modified ones **6d-e** never did. Furthermore, the donor-modified tetrakis(arylethynyl)pyrene **6a-c** were found to be stable under laboratory weathering as compared with that of coumarin. Thus, the tetrakis(arylethynyl)pyrenes **6** are expected to be applicable to bioprobes for hydrophobic pockets in various biomolecules and photomaterials.

More recently, Kim *et al.* prepared a series of alkynylpyrenes **7a-e** that bear peripheral [4-(*N,N*-dimethylamino)phenylethynyl] (DMA-ethynyl) units using pyrene as the π-center and their two-photon absorption properties (Kim et al., 2008) and electrogenerated

chemiluminescence (ECL) properties (Oh et al., 2009) were investigated in detail, respectively. These alkynylpyrenes **7a-e** showed unique patterns in photophysical and electrochemical properties. For example, compound **7e**, which has four peripheral DMA-ethynyl moieties, exhibits a marked enhancement in ECL intensity compared to the other compounds **7a-7d**; this is attributable to its highly conjugated network that gives an extraordinary stability of cation and anion radicals in oxidation and reduction process, respectively. The result is a promising step in the development of highly efficient light-emitting materials for applications such as organic light-emitting diodes (OLEDs).

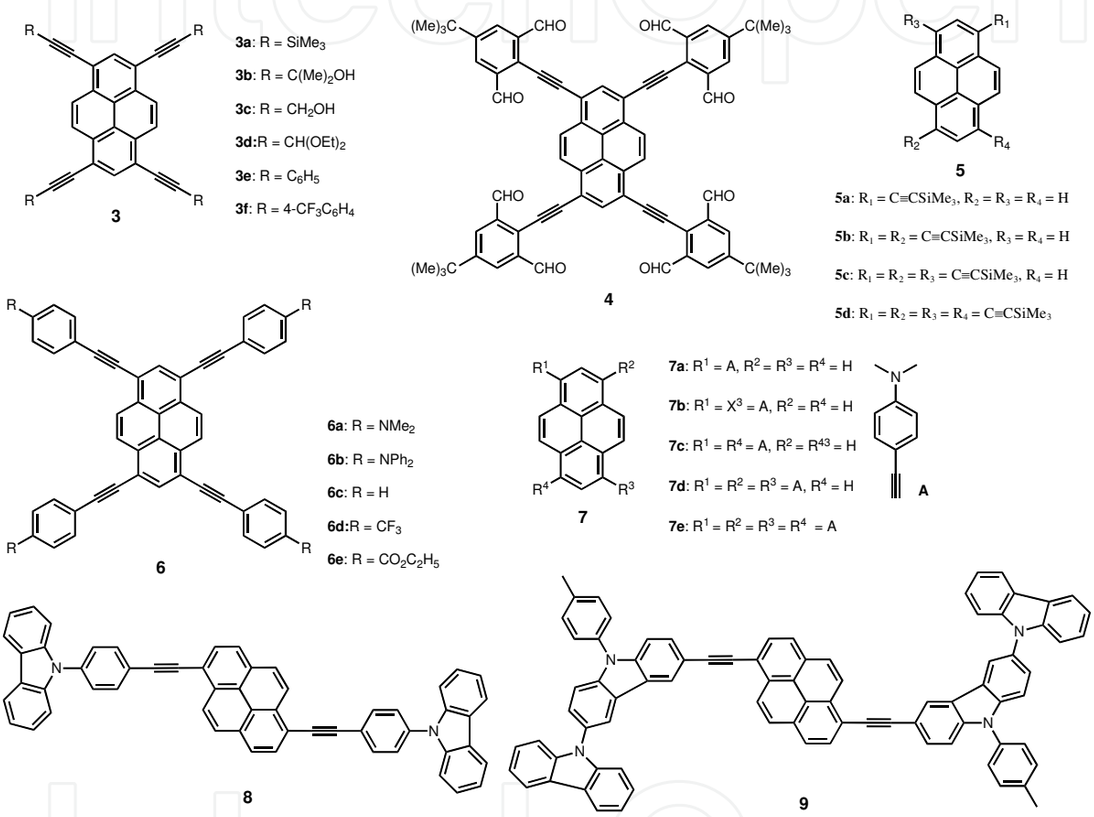


Fig. 1. Alkynyl-functionalized pyrene-cored light-emitting monomers (**3**-**9**).

Despite various alkynyl-functionalized pyrene-based light-emitting monomers with excellent efficiency and stability have been designed and studied by many research groups, there are very few examples of alkynylpyrenes-based OLED materials. Xing *et al.* (Xing et al., 2005) synthesized two ethynyl-linked carbazole-pyrene-based organic emitters (**8** and **9**, Figure 1) for electroluminescent devices. Both **8** and **9** show extremely high fluorescence quantum yield of nearly 100% because of the inserting of pyrene as electron-acceptor. Due to its higher solubility and easier fabrication than those of **8**, they fabricated a single-layer electroluminescence device by doping **9** into PVK. The single-layer device (ITO/PVK: **9** (10: 1, w/w)/Al) showed turn-on voltage at 8 V, the maximum luminance of 60 cd/m$^2$ at 17 V, and the luminous efficiency of 0.023 lm/W at 20 V. the poor performance of the device is probably due to the unbalance of electrons and holes in PVK. To improve the device performance, an additional electron-transporting layer (1,3,5-tri(phenyl-2-

benzimidazole)benzene (TPBI) was deposited by vacuum thermal evaporation in the structure of device: ITO/PVK : **9** (10 : 1, w/w) (60 nm)/TPBI (30 nm)/Al (100 nm). Physical performance of the device appeared to be improved: turn-on voltage 11 V, maximum luminance reached 1000 cd/m$^2$, external quantum efficiency was found to 0.85% at 15.5 V, and luminous efficiency was 1.1 lm/W at 15.5 V. The molecular structures of these alkynyl-functionalized pyrene-cored light-emitting monomers (**3-9**) are shown in Figure. 1.

### 3.1.2 Aryl-functionalized pyrene-cored light-emitting monomers

Recently, due to their extended delocalized π-electron, discotic shaped, high photoluminescence efficiency, and good hole-injection/transport properties, 1,3,6,8-tetrafunctional pyrene-based materials (i. e. 1,3,6,8-tetra-alkynylpyrenes and 1,3,6,8-tetraarylpyrenes) have the potential to be very interesting class of materials for opto-electronic applications. All the tetraarylpyrenes were mainly synthesized starting from the 1,3,6,8-tetrabromopyrene (**2e**). Suzuki coupling reaction between the tetrabromopyrene **2e** and the corresponding arylboronic acids or esters under Pd-catalyzed conditions afforded the corresponding tetraarylpyrenes. The first example of tetraarylpyrenes is 1,3,6,8-tetraphenylpyrene (TPPy, **10)**. TPPy is a highly efficient fluorophore showing strong blue luminescence in solution (quantum yield Φ = 0.9 in cyclohexane) (Berlamn, 1970), and the organic light emitting field-effect transistor devices (OLEFET) based on TPPy have been shown to exhibit electroluminescence (EL) with an external quantum efficiency of only 0.5% due to aggregation (Oyamada et al., 2005). In view of its high fluorescence quantum yield in solution and ease of substitution by flexible later side chains, TPPy has recently been selected as a discotic core to promote liquid-crystalline fluorescent columns. Greets and co-workers synthesized and studied several new derivatives of pyrenes (**11**) (de Halleux et al., 2004); the pyrene core has been substituted at the 1,3,6,8-positions by phenylene rings bearing alkoxy, ester, thioether, or tris(alkoxy)benzoate groups on the *para* positions. In order to generate liquid-crystalline phases, they varied the nature, number, and size of the side chains as well as the degree of polarity around the TTPy core, however, the desired liquid-crystalline behavior has not been observed. Kaszynski *et al*. (Sienkowska et al., 2007) also prepared and investigated series 1,3,6,8-tetraarylpyrenes **12** on their liquid crystalline behavior by using thermal, optical, spectroscopic, and powder XRD analysis. No mesogenic properties for these tetraarylpyrenes exhibited. Zhang and co-workers (Zhang et al., 2006) recently reported the synthesis and characterization of the first examples of novel butterfly pyrene derivatives **13** and **14**, in which thienyl and trifluoromethylphenyl aromatic groups were introduced in the 1-, 3-, 6- and 8-positions of pyrene cores through Suzuki coupling reactions of 2-thiopheneboronic acid and 4-trifluoromethylphenylboronic acid with 1,3,6,8-tetrabromopyrene (**2e**) in refluxing dioxane under a nitrogen atmosphere in good yields, respectively. The physical properties of **13** and **14** were investigated. The absorption maximum of **13**, containing electron-donating thienyl units has double absorption maximum at 314 nm and 406 nm, while **14**, with electron-withdrawing groups of trifluoromethylphenyl is located at 381 nm. The optical band gaps obtained from the absorption edges are 2.58 eV for **13** and 2.84 eV for **14**. The lower band gap for **13** is probably attributable to intramolecular charge transfer from thienyl ring to the pyrene core. Furthermore, compounds **13** and **14** exhibit strong green ($\lambda_{max}$ = 545 nm) and blue ($\lambda_{max}$ = 452 nm) fluorescence emission at longer wavelengths in the solid state than in solution ($\lambda_{max}$ = 467 nm for **13**; $\lambda_{max}$ = 425 nm for **14**; 27-78 nm red shift), indicating strong intermolecular

interaction in the solid state. The field effect transistors (FETs) device based on **14** did not show any FET performance, while the FET device using **13** as active material exhibited p-type performance. The mobility was $3.7 \times 10^{-3}$ $cm^2V^{-1}s^{-1}$ with an on/off ratio of $10^4$, and the threshold voltage was -21 V. This is the first example of a p-type FET using a butterfly pyrene-type moleculae (**13**) as the active material. More recently, a typical example of piezochromic luminescence material **15** based on TPPy was designed and prepared by Araki *et al*. (Sagara et al., 2007), in which to the *para* position of the phenyl groups of this parent molecule TPPy, four hexyl amide units were introduced as the multiple hydrogen-bonding sites. The addition of methanol to a chloroform solution of **15** resulted in precipitation of a white powder (B-form), interestingly; this blue-emitting white solid (B-form) was converted to a yellowish solid showing a strong greenish luminescence (G-form) simply by pressing it with a spatula. The absorption and fluorescence bands of **15** in chloroform solution showed structureless features at 392 and 439 nm ($\Phi$ = 0.7, life time $\tau$ = 1.3 ns), respectively, which are not much different form those of TPPy (Raytchev et al., 2003). In the solid state, the emission band of the B-form ($\Phi$ = 0.3, $\tau$ = 3.1 ns) appeared at a position similar to that in solution, but the G-Form solid showed considerable red-shifted emission at 472 nm ($\Phi$ = 0.3, $\tau$ = 3.2 ns). To clarify the different spectroscopic properties of these two solids, their solid-state structures were studied by IR spectra analysis and powder X-ray diffraction (XRD), respectively.

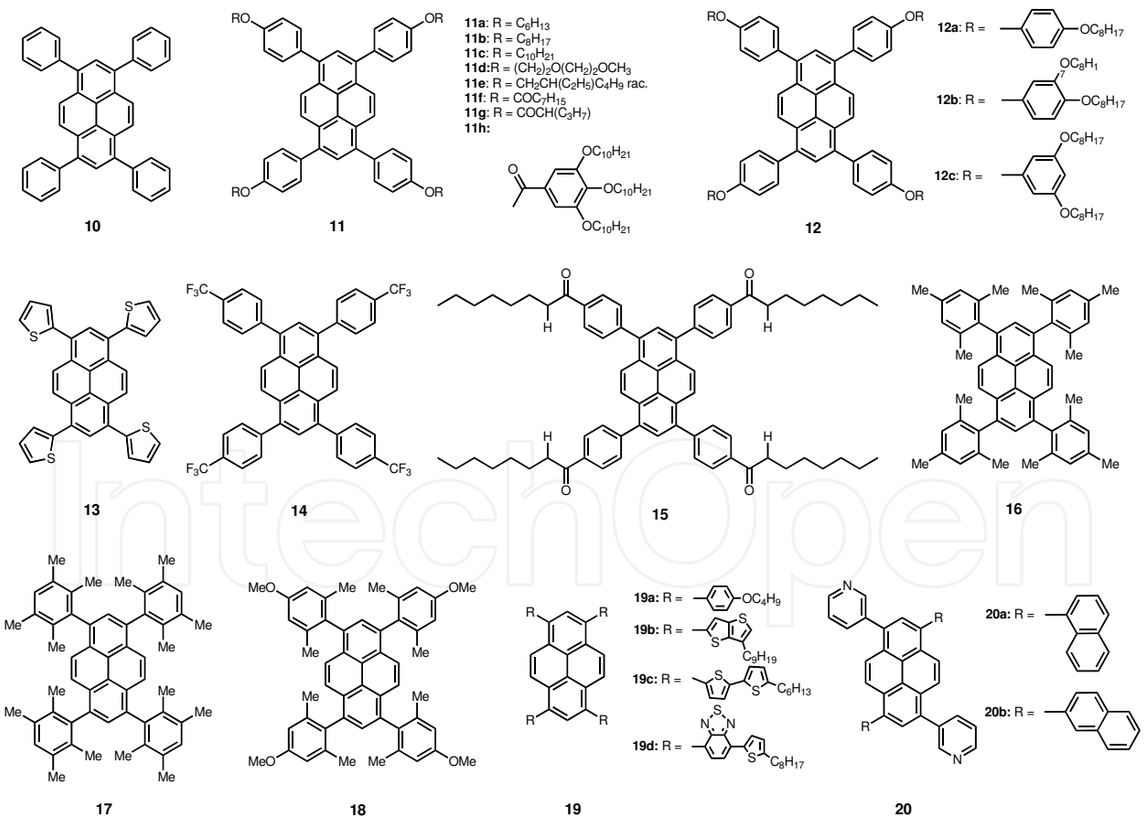


Fig. 2. Aryl-functionalized pyrene-cored light-emitting monomers (**10**-**20**).

Although the IR spectra of **15** in the B- and G-form were essentially the same, and the lower-shifted peak of the amide NH stretching at 3282 $cm^{-1}$ indicated the formation of strong

hydrogen bonds, however, closer examination of the spectra revealed that the NH stretching peak of the G-form solid was apparently broader and extended to the higher wave-number side, indicating the presence of weakly hydrogen-bonded amide units. The powder X-ray diffraction pattern of the B-form solid showed clear reflection peaks, indicating that **15** molecules in the B-form were packed in a relatively well-defined microcrystalline-like structure. On the other hand, the G-form solid did not show any noticeable diffraction in the XRD profile. The results indicated that the crystalline-like ordered structure of the B-form was disrupted in the G-form solid, agreeing well with the IR results. Therefore, the design principle in the studies could be widely applicable to other molecular systems.

As described above, numerous aryl-functionalized pyrene-cored light emitting materials have been developed, but very few of these offer OLED devices. Quite recently, several 1,3,6,8-tetraaryl-functionlized pyrenes as efficient emitters in organic light emitting diodes (OLEDs) have been reported. Moorthy *et al*. (Moorthy et al., 2007) prepared three sterically congested tetraarylpyrenes **16-18**, which can be readily accessed by Suzuki coupling between the 1,3,6,8-tetrabromopyrene (**2e**) and the corresponding arylboronic acids in isolated yields. The UV-vis absorption spectra of these arylpyrenes revealed a vibronic feature that is characteristics of unsubstituted parent pyrene with short wavelength absorption maximum at ca. 289 nm. The long wavelength absorption maximum for **16**, **17**, and **18** occurred at 363, 364, and 367 nm, respectively, which points to only a marginal difference. The photoluminescence (PL) spectra for **16-18** show that their emission maximum lie in the region between 400 and 450 nm with maximum bands at 411 nm for **16**, 412 nm for **17**, 411 nm for **18** in solutions, and at 435 nm for **16**, 434 nm for **17**, 442 nm for **18** in the solid-state, respectively. The absence of palpable red-shifted emission in all **16-18** attests to the fact that the molecules do not aggregate in the solid state to form excimers, which is also evidenced from X-ray crystal structure determination of **16**. The PL quantum yields of **16-18** in cyclohexane solution and vacuum-deposited films were found to be in the range of 0.28-0.38 and 0.24-0.44, respectively. The HOMOs and LUMOs for **16-18** vary from 5.75 to 5.80 eV and 2.56 to 2.62 eV, respectively. Thermal properties of **16-18** were gauged by thermogravimetric analysis (TGA) and differential scanning calorimetry (DSC), which were found to exhibit decomposition temperatures ($T_d$) above 300 °C and a broad endothermic melting transition ($T_m$) above 240 °C, respectively. The functional behavior of **16-18** as pure blue host emitting materials in OLEDs was investigated by fabricating devices for capturing electroluminescence (EL) as following: ITO/NPB (40 nm)/**16-18** (10 nm)/TPBI (40 nm)/LiF (1 nm)/Al (150 nm), where ITO (indium tin oxide) was the anode, NPB (*N,N'*-bis-(naphthlen-1-yl)-*N,N'*-bis(phenyl)benzidine) served as a hole-transporting layer, **16/17/18** as an emitting layer, TPBI (1,3,5-tri(phenyl-2-benzimidazole)-benzene) as an electron-transporting layer, and LiF:Al as the composite cathode. The luminance and external quantum efficiencies of the devices constructed for **16** were 1.85 cd/A and 2.2%, respectively, at a current density of 20 mA/cm$^2$ (9.48 V). The maximum luminance achieved was 3106 cd/m$^2$ with CIE of (0.15, 0.10). In contrast, the device constructed for **18** exhibited much better performance yielding a maximum external quantum efficiency of ca. 3.3% at 6.5 V. The maximum luminance efficiency achieved was 2.7 cd/A at a current density of 5.25 mA/cm$^2$ (6.5) with a maximum luminance of 4730 cd/m$^2$ with CIE of (0.14, 0.09). Thus, the maximum external efficiency achieved for the non-doped blue emitting device fabricated for **18** is 3.3%; this value is comparable to commonly used blue emitting materials based on spirofluorene (3.2 cd/A) (Kim et al., 2001), diarylanthracences (2.6-3.0 cd/A) (Kim et al., 2005; Tao et al., 2004), diphenylvinylbiphenyls (1.78 cd/A) (Xie et al., 2003), biaryls

(4.0cd/A) (Shih et al., 2002), etc. The maximum luminance efficiency of 2.7 cd/A achieved in **18** underscores the fact that the attachment of sterically hindered substituents to the pyrene does indeed lead to suppression of face-to-face aggregation.

Small molecules advantageous because they can be i) purified by column techniques such as recrystalliztion, chromatography, and sublimation and ii) vacuum-deposited in multilayer stack both important for device lifetime and efficiency (Anthony et al., 2008). However, vacuum-deposition techniques require costly processes that are limited to practical substrate size and relatively low yields in the manufacture of high volume products using masking technologies (Shtein et al., 2004). On the other hand, polymers are generally of lower purity than small molecules but can be used to achieve larger display sizes at much lower costs using technologies such as inkjet and screen printing (Krebs, 2009; Loo & McCulloch, 2008; Sirringhaus & Ando, 2008). By combining the advantages of both small molecules and polymers, specially, 1,3,6,8-tetraarylpyrenes (**19**) with high purity and solution processability for application in organic electronics was recently reported by Sellinger and co-workers (Sonar et al., 2010), which were synthesized by both Stille and Suzuki-Miyaura cross coupling, respectively. All compounds **19a-d** are readily soluble in common organic solvents such as $CHCl_3$, $CH_2Cl_2$, THF and toluene, which allows for purification by column chromatography and solution processing. The photophysical properties of **19** were measured by UV-vis absorption and photoluminescence (PL) spectroscopy in chloroform and in thin films. Compounds **19a** and **19d** show red-shifted wavelength absorption maximum ($\lambda_{max}$) at 451 and 452 nm in comparison to **19b** and **19c** ($\lambda_{max}$ = 394 and 429 nm, respectively) due to their slightly more extended conjugation lengths. In thin film absorption, compounds **19a**, **19c**, and **19d** show red shifts of ca. 13-19 nm, while **19b** shows similar absorbance compared to their respective dilute solutions. Solution PL spectra of **19b** and **19c** show deep blue and sky blue emission, respectively, at 433 and 490 nm, whereas **19a** and **19d** exhibit green and orange emission at 530 and 541 nm, respectively. In thin film PL, all compounds **19** are red-shifted 29-95 nm compared their corresponding solutions due to aggregation in the solid state. The calculated HOMO values for **19** are in range of 5.15 to 5.33 eV, these energy levels match quite with commonly used hole injection/transport layer and anodes such as PEDOT: PSS (5.1 eV) and ITO (4.9 eV), indicating the materials are suitable for application in OLEDs. The strong PL emission, tunable energy levels, excellent solubility, enhanced thermal properties, and good film-forming properties make these materials promising candidates for application in solution-processed devices. Using **19b** as a potential deep blue emitting material, a structure of the OLED is fabricated as following: indium tin oxide (ITO)/PEDOT: PSS (50 nm)/**19b** (50 nm)/1,3,5-tris(phenyl-20benzimidazolyl)-benzene (TPBI) (20 nm)/Ca (20 nm)/Ag (100 nm) where PEDOT/PSS and TPBI act as hole-injecting/transport and electron-injecting/transport layers, respectively. The maximum brightness and luminance efficiency are 5015 cd/m$^2$ (at 11 V) and 2.56 cd/A (at 10 cd/m$^2$) with CIE coordinates (0,15, 0.18), respectively. The efficiency numbers are quite promising for unoptimized small molecule solution processed blue OLEDs (Zhang et al., 2010; Wang et al., 2009). The turn-on voltage for the device of around 3 V is quite low, suggesting that the barrier for hole injection from PEDOT: PSS is low, which is expected from the measured HOMO level of **19b**.

For OLEDs, to achieve maximum device efficiency is highly depended on the balance of carrier recombination, because the hole mobility is usually much higher than the electron mobility under the same electric field (Chen et al., 1999; Chu et al., 2007). And thus, emitting and charge-transporting materials with a high ionization potential values such as oxadiazole

(Tokito et al., 1997), benzimidazole (Shi et al., 1997), diarylsilole group materials (Uchida et al., 2001) and electron transport materials (ETMs) (Kulkarni et al., 2004; Strohriegl & Grazulevicius, 2002) were synthesized and applied to OLEDs. On the other hand, the polycyclic aromatic hydrocarbons such as naphthalenes, anthracenes, and pyrenes, compared with hetero-aromatic compounds, are known to be not suitable for ETMs due to their high reduction potentials, but they have good thermal stability and no absorption at longer wavelengths than 430 nm (Tonzola et al., 2003). Among them, pyrene has relatively high electron affinity values and better thermal stability. Lee an co-workers (Oh et al., 2009) synthesized new kinds of pyrene-based electron transport materials (ETMs): 1,6-di(pyridin-3-yl)-3,8-di-(naphthlen-1-yl)pyrene (**20a**) and 1,6-di(pyridin-3-yl)-3,8-di(naphthlen-2-yl)pyrene (**20b**) *via* Suzuki coupling reaction starting from 1,6-dibromopyrene (**2b**). Three blue OLEDs (**1-3**) were fabricated by high-vacuum thermal evaporation of OLED materials on to ITO-coated glass as following: ITO/DNTPD (60 nm)/NPB (30 nm)/AND: TBP 3wt% (25 nm)/$Alq_3$ (device **1**) or **20a** (device **2**) or **20b** (device **3**) (25 nm)/LiF (0.5 nm)/Al (100 nm), where 4,4′-bis[*N*-[4-{*N,N*-bis(3-methylphenyl)amino}-phenyl]-*N*-phenylamino]biphenyl (DNTPD) and 4,4′-bis[*N*-(1-naphthyl)-*N*-phenylamino] biphenyl (NPB) act as hole-injecting/transport layers (HTL), AND : TBP 3wt% act as emitting layers (EML), and $Alq_3$ or **20a** or **20b** act as electron-injecting/transport layers (ETL), respectively. The external quantum efficiencies of the devices **2-3** with the newly-developed pyrene-based molecules **20a/20b** as electron transport materials increase by more than 50% at 1 mA $cm^{-2}$ compared with those of the device **1** with representative $Alq_3$ as an electron transport material. The enhanced quantum efficiencies are due to the balanced charge recombination in an emissive layer. Electron mobilities in **20a** and **20b** films are 3.7 x $10^{-5}$ $cm^2$ $(Vs)^{-1}$ and 4.3 x $10^{-5}$ $cm^2$ $(Vs)^{-1}$, respectively. These values are three times higher than that of $Alq_3$. Highly enhanced power efficiency is achieved at 1.4 lm/W for device **1** with $Alq_3$, 2.0 lm/W for device **2** with **20a**, and 2.1 lm/W for device **3** with **20b** at 2000 cd/$m^2$ due to a low electron injection barrier and high electron mobility. All structures for these 1,3,6,8-tetraaryl-functionalized pyrene-cored light-emitting monomers (**10-20**) are shown in Figure. 2.

### 3.2 Pyrenyl-functionalized PAHs-cored light-emitting monomers

Due to the most attractive features of its excimer formation, delayed fluorescence, rather fluorescence lifetimes, etc., pyrene is also a fascinating subchromophores for constructing highly efficient fluorescent light-emitting monomers for OLEDs applications. Recent literatures survey revealed that there are many number of investigations concerning the attachment of pyrene to other aromatic fluorophores such as benzene, fluorene, and carbazole, etc. as highly efficient emitters in OLEDs. In this section, the synthesis and photophysical properties of three types of pyrenyl-functionalized PAHs-cored light-emitting monomers were summarized. Especially, several these light-emitting monomers as emitters in efficient OLEDs will be fully discussed.

#### 3.2.1 Pyrenyl-functionalized benzene-cored light-emitting monomers

Hexaarylbenzenes have received much attention in material science in recent years (Rathore et al., 2001; Rathore et al., 2004; Sun et al., 2005) for application as light emitting and charge-transport layer in OLEDs (Jia et al., 2005). Lambet *et al*. (Rausch & Lambert, 2006) designed a synthetic route to the first hexapyrenylbenzene **21** starting from 4,5,9,10-tetrahydropyrene, in which six pyrenyl substituents are arranged in a regular manner and held together by a

central benzene core. The absorption spectrum of **21** in dichloromethane shows the typical allowed bands at 465 and 398 nm, and the much weaker forbidden bands at 347 and 280 nm, respectively, which display vibronic structure and are distinctly shifted to lower energy region. The emission spectrum of **21**, peaked at 415 nm, also shows a vibronic fine structure but is much less resolved than that of the parent pyrene. At the low-energy side, there is a broad and unresolved shoulder at 483 nm, which is more intense in polar solvents than in moderately or apolar solvents. The emission spectrum is independent of the concentration such that excimer formation between two molecules of **21** could be excluded, which is both from locally excited pyrene states and from the excitonic states of the aggregate. The others pyrenyl-functionalized benzenes such as 1,3,5-tripyrenyl-functionalized benzenes (**22**) and dipyrenylbenzens (**23**), as organic luminescence (EL) lighting materials are recently disclosed by many patents (Charles et al., 2005; Cheng & Lin, 2009). For example, 1,3,5-tripyrenylbenzene **22**, this arrangement results in a good blue emissive material with a peak emission at 450 nm. However, the compound still has a minor aggregation problem in its solid state, resulting in a shoulder emission at 482 nm and reduced blue color purity. More recently, Sun and co-workers (Yang et al., 2007) reported the synthesis of dipyrenylbenzenes (**24** and **25**) as the light emissive layer for highly efficient organic electroluminescence (EL) diodes. The UV-vis absorption of **24** and **25**, in chloroform, shows the characteristic vibration pattern of the pyrene group at 280, 330 and 349 nm for **24**, 281 and 352 nm for **25**, respectively. Upon excitation, the PL spectra with $\lambda_{max}$ = 430, 426 nm are observed and the full-widths at half-maximum (FWHM) of **24** and **25** are 63 and 64 nm, respectively. To study the EL properties of **24** and **25**, multilayer devices with the configuration of ITO/NPB (50 nm)/**24** or **25** (30 nm)/BCP (10 nm)/$Alq_3$ (30 nm)/LiF (1 nm)/Al were fabricated. For device with **24**, the maximum intensity is located at 488 nm with the CIE coordinates of (0.21, 0.35). The color of the emission is bluish green, covering the visible region of 420-600 nm, which probably due to the injected charge carriers are recombined at NPB layer, results in broadening the EL spectrum for this device. For device with **25**, EL emission is centered at 468 nm and the CIE coordinates are (0.19, 0.25). The best power efficiency obtained for the **24** device and the **25** device was 4.09 lm/W at a voltage, current density, and luminance of 5.6 V, 20 mA/cm$^2$, and 1459 cd/m$^2$, and 5.18 lm/W at a voltage, current density, and luminance of 5.2 V, 20 mA/cm$^2$, and 1714 cd/m$^2$, respectively. Another examples of dipyrenylbenzene derivatives, 1-(4-(1-pyrenyl)phenyl)pyrene (**PPP**, **26a**), 1-(2,5-dimethoxy-4-(1-pyrenyl)-phenyl)pyrene (**DOPPP**, **26b**), and 1-(2,5-dimethyl-4-(1-pyrenyl)phenyl)pyrene (**DMPPP**, **26c**) have been recently reported by Cheng *et al*. (Wu et al., 2008), which was synthesized by the Suzuki coupling reaction of aryl dibromides with pyreneboronic acid. These compounds exhibit high glass-transition temperatures ($T_g$) at 97 $^o$C for **PPP**, 135 ˚C for **DOPPP**, and 137 ˚C for **DMPPP**, respectively. The lower $T_g$ of **PPP** is probably because of the low rotations barrier of the central phenylene group in **PPP** compared with that of substituted phenylene group in **DOPPP** and **DMPPP**. Single-crystal X-ray analysis revealed that these dipyrenylbenzenes adopt a twisted conformation with inter-ring torsion angles of 44.5°-63.2° in the solid state. Thus, The twisted structure is responsible for the low degree of aggregation in the films that leads to fluorescence emission of the neat films at 446-463 nm, which is shorten than that of the typical pyrene excimer emission, and also conductive for the observed high fluorescence quantum yields of 63-75 %. The absorption spectra for **PPP**, **DOPPP** and **DMPPP** in dilute dichloromethane solutions (< $10^{-4}$ M) showed vibronic structures typical for the pyrene moiety at 300-350 nm.

The PL spectra of **PPP** and **DOPPP** have lost vibronic structure and red-shifted to 428-433 nm with respect to the pyrene monomer emission, while the **DMPPP** emission centered at 394 nm still maintains a weak vibronic feature. On the other hand, the absorption spectra of these thin-film samples show a broad band at 354-361 nm, which is red-shifted by approx. 10 nm relative to those in solution. The PL spectra of **PPP**, **DOPPP**, and **DMPPP** are red-shifted by 18-52 nm to 463, 451, and 446 nm, respectively and become broader with a FWHM of 68-78 nm from dichloromethane solution to the thin-film state. Such red-shifts could be attributed to i) the aggregation of pyrene groups and ii) the extension of π-delocalization caused by the more coplanar configuration (An et al., 2002) of these dipyrenylbenzenes (**26**) in the neat film. A bilayer device using PPP as the hole transporter and $Alq_3$ as the emitter emits green light at 513 nm from the $Alq_3$ emitter, which can comparable to the common $Alq_3$-based devices using NPB as the hole transporter, indicating **PPP** is an excellent hole transporter. Furthermore, three devices consists of [ITO/CuPc (10 nm)/NPB (50 nm)/**PPP** or **DOPPP** or **DMPP** (30 nm)/TPBI (40 nm)/ Mg:Ag/Ag] were fabricated, where CuPc act as a hole injecter, TPBI act as a hole blocker and electron transporter, respectively. **PPP**-based device emits blue light at 474 nm efficiently with a maximum $\eta_{ext}$ of 4.5 % and CIE coordinates of (0.14, 0.20); at a current density of 20 mA/cm$^2$, the luminance and the $\eta_{ext}$ are 1300 cd m$^{-2}$ and 4.2 %, respectively. In particular, **DOPPP**-based device emits blue light at 455 nm efficiently with a maximum $\eta_{ext}$ of 4.3 % and CIE coordinates of (0.15, 0.16); at a current density of 20 mA/cm$^2$, the luminance and the $\eta_{ext}$ are 980 cd m$^{-2}$ and 3.7 %, respectively. **DMPPP**-based device emits deep-blue light at 446 nm with CIE coordinates of (0.15, 0.11), the maximum $\eta_{ext}$ and luminance reach as high as 5.2 % and 40400 cd m$^{-2}$ (14 V), respectively, at 20 mA cm$^{-2}$, the luminance and $\eta_{ext}$ are 902 cd m$^{-2}$ and 4.4 %, respectively. All chemical structures of these pyrenyl-functionalized benzenes are show in Figure. 3.

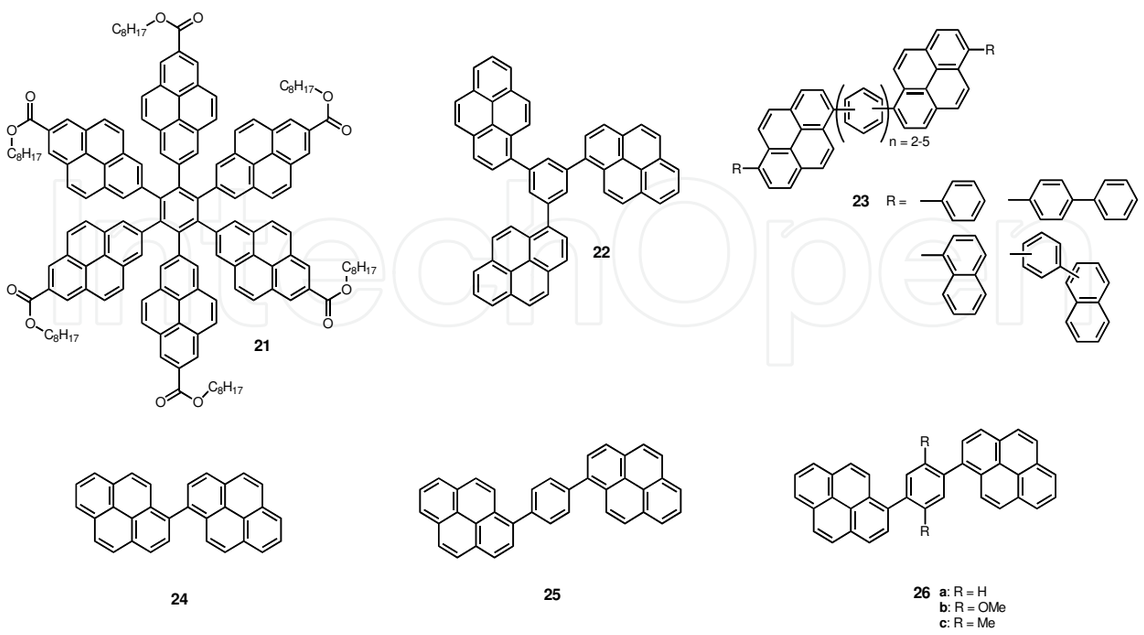


Fig. 3. Pyrenyl-functionalized benzene-cored light-emitting monomers (**21**-**26**).

### 3.2.2 Pyrenyl-functionalized fluorene-cored light-emitting monomers

Because of their high photoluminescence (PL) efficiency, much research into blue-emitting materials has focused on conjugated fluorene derivatives (Yu et al., 2000; Wong et al., 2002; Kim et al., 2001), and further the introduction of aryl groups at C9 position of fluorene could improve the stability of the materials. On the other hand, as a large conjugated aromatic ring, pyrene has the advantages of high PL efficiency, high carrier mobility, and the much improved hole-injection ability than oligofluorenes or polyfluorene (Tao et al., 2005). Thus, the combination of the high thermal stability of diarylfluorene with the high efficiency and hole-injection ability of pyrene is expected to develop new blue-light-emitting materials for OLEDs applications. Recently, some fluorene derivatives that functionalized by pyrenyl groups at 2-, and 7-positions have been used in OLEDs. Tao *et al*. (Tao et al., 2005) reported the synthesis and characterization of a series of fluorene detivatives, 2,7-dipyrene-9,9′-dimethylfluorene (**27**, **DPF**), 2,7-dipyrene-9,9′-diphenylfluorene (**28**, **DPhDPF**), and 2,7-dipyrene-9,9′-spirobifluorene (**29**, **SDPF**), in which pyrenyl groups are introduced because they are highly emissive, bulky, and rigid, and thus expected to improve the fluorescence quantum yields and thermal stability of the fluorene derivatives. The fluorene derivatives (**27-29**) have high fluorenscence yields (0.68-0.78, in $CH_2Cl_2$ solution), good thermal stability (stable up to 450 ˚C in air), and high glass-transition temperatures in the range of 145-193 ˚C. All UV-vis absorption spectra of **DPF**, **DPhDPF**, and **SDPF** in dilute $CH_2Cl_2$ solution exhibits the characteristic vibration pattern of the isolated pyrene groups with maximum peaks at 360 nm for **DPF**, 362 nm for **DPhDPF**, and 364 nm for **SDPF**, respectively. The PL spectrum of the **DPF**, **DPhDPF**, and **SDPF** and films shows blue emission peaks at 421, 422, and 422 nm in solution, and 460, 465, and 465 nm in films, respectively. The shifts are probably due to the difference in dielectric constant of the environment (Salbeck et al., 1997). Using the three derivatives as host emitters, Blue-light-emitting OLEDs were fabricated in the configuration of ITO/CuPc ( 15 nm)/NPB ( 50 nm)/**DPF** or **DPhDPF** or **SDPF** (30 nm)/$Alq_3$ (50 nm)/Mg:Ag (200 nm). Among them, the turn-on voltage of the **DPF**-based device is 5.8 V and the device achieves a maximum brightness of 14300 cd/m² at a voltage of 16 V and a current density of 390 mA/cm² with CIE coordinates of (0.17, 0.24). The maximum current efficiency of the blue OLEDs made with **DPF**, **DPhDPF**, and **SDPF** host layers is 4.8, 5.0, and 4.9 cd/A, respectively. To confine and enhance electron-hole recombination in the EML and thus to increase device efficiency, a hole-blocking layer, such as a layer of 2,2′,2″-(benzen-1,3,5-triyl)tris(1-phenyl-1*H*-benzimidazole) (TPBI) is commonly used between the EML and ETL. Thus, a modified device with a configuration: ITO/CuPc (15 nm)/NPB (50 nm)/**DPF** ( nm)/TPBI (50 nm)/Mg:Ag was fabricated Compared to the $Alq_3$-based device, the TPBI-based device indeed shows a higher efficiency of 5.3 cd/A and 3.0 lm/W, and better CIE coordinates of (0.16, 0.22) with a lower turn-on voltage of 5.2 V.

Along this line, Huang and co-workers (Tang et al., 2006) also designed and synthesized two highly efficient blue-emitting fluorene derivatives, 2-pyrenyl-9-phenyl-9-pyrenylfluorene (**30a**, $\mathbf{P_1}$) and 2,7-dipyrenyl-9-phenyl-9-pyrenyl-fluorene (**30b**, $\mathbf{P_2}$). They fabricated devices of ITO/TCTA (8 nm)/$\mathbf{P_1}$ or $\mathbf{P_2}$ (30 nm)/BCP (40 nm)/Mg: Ag, where the TCTA (4,4′,4″,-tri(*N*-carbazolyl)triphenylamine) was used as both the buffer layer and hole-transporting layer, and BCP (2,9-dimethyl-4,7-diphenyl-1,10-phenanthroline) as both the buffer layer and electron-transporting layer. The devices have low turn-on voltages of 4 and 3.5 V, with high current efficiencies of 2.56 (9.5 V) and 3.08 cd/A (9 V), high power efficiencies of 0.85 and 1.17 lm/W (7.5 V), and high brightness of 16664 (15 V) and 19885 cd/m² (13 V) for $\mathbf{P_1}$-based device and $\mathbf{P_2}$-based device, respectively. The peaks of the blue EL spectra were all at 454

nm with CIE coordinates of (0.17, 0.17) and (0.17, 0.19) for $\mathbf{P_1}$-based device and $\mathbf{P_2}$-based device, respectively. In order to obtain a better solubility and a low tendency to crystallize in devices, a long chain alkyloxy group was introduced into C9 phenyl at *para*-position, two new efficient blue-light-emitting materials, 2-pyrenyl-9-alkyloxyphenyl-9-pyrenylfluorene (**31a**) and 2,7-dipyrenyl-9- alkyloxyphenyl-9-pyrenylfluorene (**31b**) have also been reported by Huang's group (Tang et al., 2006). A preliminary simple three layer blue-light-emitting diodes with a configuration of ITO/TCTA (8 nm)/**31a** (30 nm)/BCP (45 nm)/Mg:Ag, was fabricated and obtained without the need for a hole-injection layer, with high luminance of 11620 cd/m² (14.6 V), turn-on voltage of 4.0 V, current efficiency of 3.04 cd/A (8.8 V) and CIE coordinates of (0.18, 0.23). More recently, two solution-processable, pyrenyl-functionalized, fluorene-based light emitting materials, 2-(1-ethynylpyrenyl)-9-alkyloxyphenyl-9-pyrenylfluorene (**32a**) and 2,7-di(1-ethynyl-pyrenyl)-9- alkyloxyphenyl-9-pyrenylfluorene (**32b**) were reported by Huang's group (Liu et al., 2009). They emit blue light in solution and green light in film at 412, 439 nm and 514, 495 nm, respectively. Because of the good thermal stability and excellent film-forming ability, **32a** was chosen as the active material in solution processed devices. Two single layered devices with the configurations of [ITO/PEDOT: PSS (40 nm)/**32a** (80 nm)/Ba (4 nm)/Al (120 nm)] (Device 1) and [ITO/PEDOT: PSS (40 nm)/**32a** (80 nm)/CsF (4 nm)/Al (120 nm)] (Device 2) were fabricated. For device 1, it showed bright green emission with peak at 522 nm with CIE coordinate of (0.36, 0.54). The turn-on voltage was 4.2 V, the maximum brightness was 3544 cd/m² and the maximum current efficiency reached 0.9 cd/A. For device 2, it showed bright green emission with peak at 528 nm with CIE coordinate of (0.39, 0.54). The turn-on voltage was 3.2 V, the maximum brightness was 8325 cd/m² and the maximum current efficiency reached 2.55 cd/A. The results suggest that for pyrene-based materials, CsF was a more efficient cathode than barium in electron injection. This was because the Ba was still an injection limited cathode for **32a**, While the presence of Al capping cathode, free low work function alkali metal would be generated at the **32a**/CsF interface and the CsF layer produced an interfacial dipole. Another solution processable, pyrenyl-functionalized

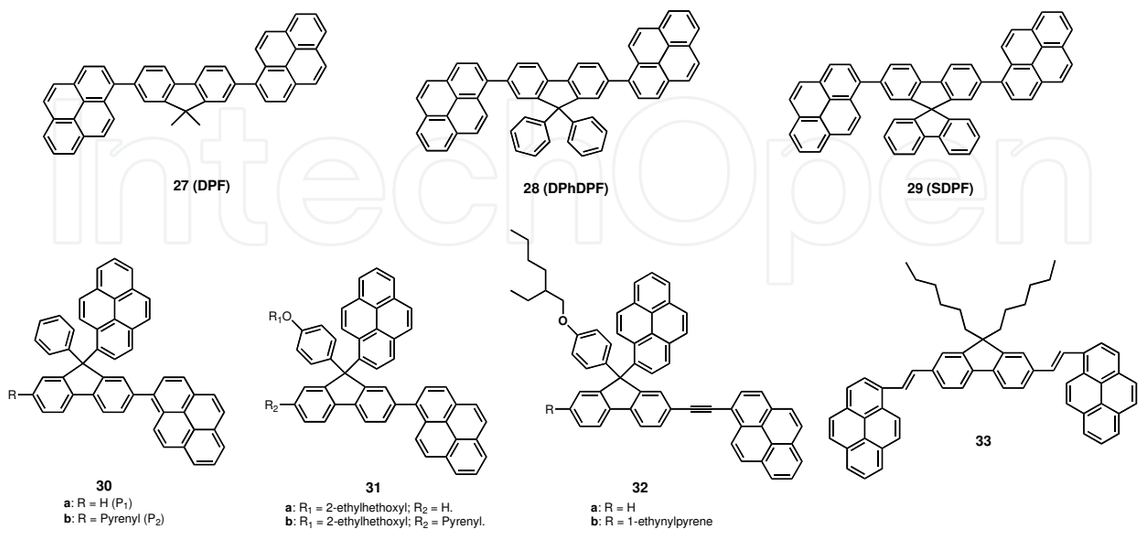


Fig. 4. Pyrenyl-functionalized fluorene-based light-emitting monomers (**27**-**33**).

fluorene-based light-emitting material (**33**) was reported by Adachi and co-worker (Mikroyannidis et al., 2006), which was carried out by the Heck coupling reaction of 9,9-dihexyl-2,7-divinylfluorene with 1-bromopyrene (**2a**). However, very poor EL efficiency of $\eta_{EL} \sim 10^{-5}\%$ at 30 V was observed in the OLED device with **33**, which might due to both unbalanced hole and electron injection, and the interior film quality of the **33** layer. The structures of the pyrenyl-functionalised fluorene-based light-emitting monomers are shown in Figure 4.

### 3.2.3 Carbazole/arylamine/fluorene/pyrene-composed hybrids light-emitting monomers

Performance of the Organic EL device significantly affects by the charge balance between electrons and holes from opposite electrodes. One useful and simple approach of balancing the rates of injection of electrons and holes employs a bilayer structure comprising a hole-transport layer and an electron-transport layer, with one or both being luminescent (Chen et al., 1998). Another extremely important issue of organic EL materials is their durability (i.e. thermal and morphological stability). It is well demonstrated that the thermal stability or glass-state durability of organic compounds could be greatly improved upon incorporation of a carbazole or fused aromatic moiety in the core structure (Kuwabara et al., 1994; Koene et al., 1998; O'Brien et al., 1998). Furthermore, the carbazole moiety can be easily functionalized at its 3-, 6-, or 9-positions and covalently linked to other molecular moieties (Joule, 1984), such as alkyl, phenyl, diarylamine, pyrenyl, etc. Similarly, the fluorene molecule can also be easily functionalized at its 2-, 7-, and 9-positions (Lee et al., 2001; Zhao et al., 2006). Therefore, thermally and morphologically stable hybrids possessing dual functions, high light emitting and hole transporting, should be available by composing the carbazole, fluorene, and pyrene, etc. Thomas and co-workers (Thomas et al., 2000) firstly reported the synthesis of the carbazole/arylamine/pyrene-composed hybrids (**34-36**, Figure. 5) by palladium-catalyzed amination of 3,6-di-bromocarbazole, and the use of the resulting hybrids in OLEDs fabrication. As expected, for these compounds **34-36**, both high decomposition temperatures ($T_d$ > 450 ˚C) and rather high glass transition temperatures ($T_g$ = 180-184 °C) were obtained, which may offer improved lifetime in devices. Double-layer EL devices of ITO/**34** (40 nm)/TPBI (40 nm)/Mg: Ag were fabricated using compound **34** as the hole-transport layer as well as the emitting layer and TPBI as the electron-transport layer. Green light emission at 530 nm was observed and the physical performance appears to be promising: turn-on voltage 5 V, maximum luminescence (38000 cd/m$^2$) at 13.5 V, external quantum efficiency of 1.5 % at 5 V, and luminous efficiency of 2.5 lm/W at 5V, which are in general better than those of typical green-light-emitting devices of ITO/diamine/$Alq_3$/Mg: Ag (Kido et al., 1997). Similar results were also obtained in preliminary studies of the devices with **35** and **36**. Another series of carbazole/arylamine/pyrene-composed hybrids (**37a-c**, Figure 5) were also prepared and reported by Thomas *et al*. in their follow-up works (Thomas et al., 2001). The UV-vis absorption spectra of **37** display bands resulting from the combination of carbazole and pyrene chromophores and cover the entire UV-vis region (250-450 nm). All the compounds emit green light at 548 nm for **37a**, 515 nm for **37b**, and 537 nm for **37c** in $CH_2Cl_2$ solution, while a significant blue-shift (25 nm for **37a**, 6 nm for **37b**, and 26 nm for **37c**) in the corresponding film states and bandwidth narrowing were observed, indicating the sterically demanding bulky pyrenyl substituents prevent the close packing in the solid state. Using

these compounds as both hole-transport and emitting materials, two types of double-layered EL devices were fabricated: (I) ITO/**37**/TPBI/Mg: Ag; (II) ITO/**37**/$Alq_3$/Mg: Ag. In the type I devices with TPBI as ETL, emissions from the hybrids **37** were observed at 516 nm for **37a**, 500 nm for **37b**, and 500, 526 nm for **37c**, respectively, as suggested from a close resemblance of the EL and the PL of the corresponding compounds **37**. In the type II devices with $Alq_3$ as ETL, again the emission from the compounds **37** layer was found at 516 nm fro **37a**, 500 nm for **37b**, and 502, 528 for **37c**, respectively. While the devices are not optimized, the physical performance appears to be promising: maximum luminescence (**37a**, 41973 cd/m² at 14.0 V; **37b**, 48853 cd/m² at 13.5 V; **37c**, 33783 cd/m² at 14.5 V), maximum external quantum efficiency (**37a**, 1.66 % at 6.0 V; **37b**, 2.19 % at 4.0 V; **37c**, 1.74% at 4.0 V), and maximum luminous efficiency (**37a**, 3.88 lm/W at 4.0 V; **37b**, 4.77 lm/W at 3.5 V; **37c**, 5.68 lm/W at 3.0 V). Thus, the EL devices based on the compounds **37** are also better than those of typical green-light-emitting devices of ITO/diamine/$Alq_3$/Mg: Ag (Kido & Lizumi, 1997). Very recently, Pu and co-workers (Pu et al., 2008) reported a fluorene/arylamine/pyrene-composed fluorescent hybrid (**38**, Figure 5) as solution processable light-emitting dye in organic EL device, which was synthesized by palladium-catalysed cross-coupling reaction between 2-(2′-bromo-9′,9′-diethylfluoren-7′-yl)- 9,9-diethylfluorene and 1-aminopyrene. Light emitting devices with the configuration of ITO/PEDOT: PSS (40 nm)/**38** (50 nm)/BAlq (50 nm)/LiF (0.5 nm)/Al (100 nm) were fabricated. PEDOT: PSS and the emitting layer (**38**) were deposited by spin-coating in open atmosphere. BAlq (4-phenylphenolato)aluminium(III)) was deposited by evaporation under vacuum act as a hole blocking layer. The device emits a yellow light at 572 nm, the turn-on voltage, current efficiency, luminance efficiency, and $\eta_{ext}$ are 6.07 V, 1.42 lm/W, 2.75 cd/A, and 0.93% at 100 cd/m², respectively; the turn-on voltage, current efficiency, luminance efficiency, and $\eta_{ext}$ are 8.65 V, 0.75 lm/W, 2.07 cd/A, and 0.71% at 1000 cd/m², respectively.

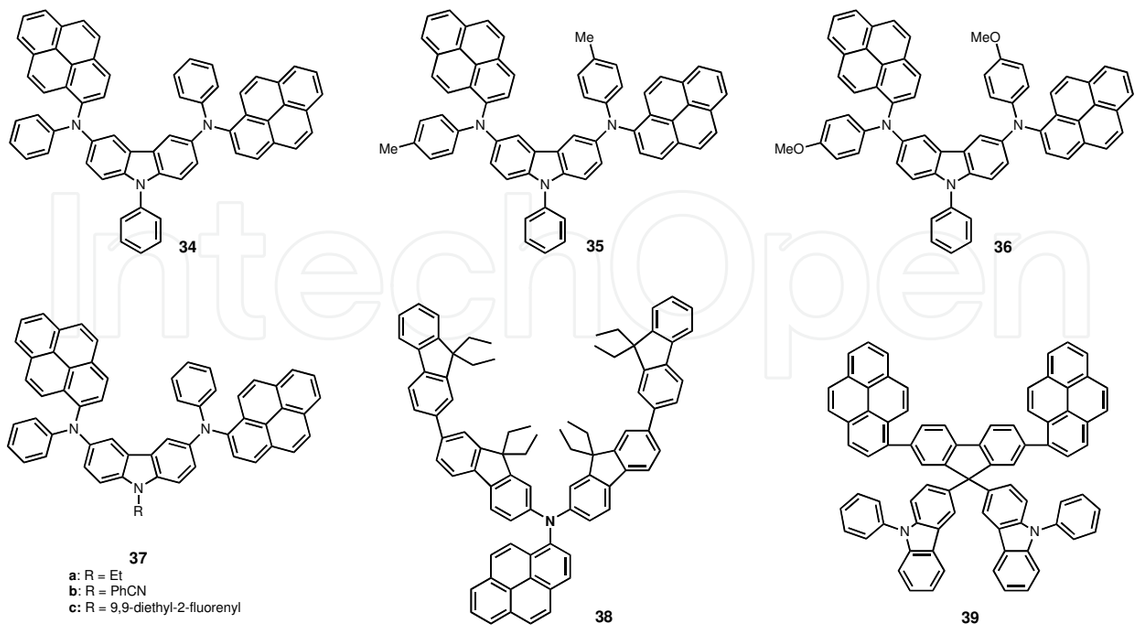


Fig. 5. Carbazole/arylamine/fluorene/pyrene-composed hybrids light-emitting monomers (**34**-**39**).

Quite recently, Tao *et al*. (Tao et al., 2010) reported the synthesis and characterization of a new carbazole/fluorene/pyrene-composed organic light emitting hybrids, 9,9-bis-(3-9-phenyl-carbazoyl)-2,7-dipyrenylfluorene (**39**). Using 39 as a emitter, a nondoped device with typical three-layer structure of ITO/NPB (50 nm)/**39** (20 nm)/TPBI (30 nm)/LiF (0.5 nm)/MgAg (100 nm) was fabricated. The device exhibits deep-blue emission with a peak centered at 458 nm and CIE coordinates of (0.15, 0.15). The devices shows a turn-on voltage (at 1 cd/m$^2$) of < 3.5 V and achieves a maximum brightness of 7332 cd/m$^2$ at a voltage of 9 V and a current density of 175 mA/cm$^2$, the maximum current efficiency of 4.4 cd/A (at 3.1 lm/W). The results indicate that introduction of carbazole units at the 9-position of fluorene is an efficient means for reducing red shift of the emission from molecular aggregation. Furthermore, the chemical structures for the carbazole/arylamine/ fluorene/pyrene-composed hybrids light-emitting monomers are show in Figure. 5.

## 4. Functionalized pyrene-based light-emitting dendrimers

Dendrimers are hyperbranched macromolecules that consist of a core, dendrons and surface groups (Newkome et al., 1996). Generally light-emitting dendrimers consist of a fluorescent light-emitting core to which one or more branched dendrons are attached. Furthermore, light-emitting dendrimers possess many potential advantages over conjugated polymers and small molecule materials. First, their key electronic properties, such as light emission, can be finely tuned by the selection of the core drawing from a wide range of luminescent chromophores, including fluorescent groups and phosphorescent groups. Second, by selecting the appropriate surface groups, solubility of the molecule can be adjusted. Finally, the level of intermolecular interactions of the dendrimers can be controlled by the type and generations of the dendrons employed, that are vital element to OLEDs performance. Recently, several types of fluorescent light-emitting dendrimers (Wang et al., 1996; Halim et al., 1999; Freeman et al., 2000; Adronov et al., 2000; Lupton et al., 2001; Kwok & Wong, 2001) and phosphorescent light-emitting dendrimers (Lo et al., 2002, 2003; Markham et al., 2004; Ding et al., 2006) have been disclosed in recent literatures that successfully used in the fabrication of OLEDs by means of solution process. For example, Ding and co-workers have developed a class of phosphorescent iridium dendrimers based on carbazole dendrons (Ding et al., 2006), with a device structure of ITO/PEDOT: PSS/neat **dendrimers**/TPBI/LiF/Al, a maximum external quantum efficiency (EQE) of 10.3 % and a maximum luminous efficiency of 34.7 cd A$^{-1}$ are realized. By doping these dendrimers into carbazole-based host, the maximum EQE can be further improved to 16.6%.

On the other hand, substitution in the pyrene core at the most active centers (i.e. 1-, 3-, 6-, and 8-positions) exclusively by the dendrons can lead to interesting dendritic architectures with a well-defined number of chromophores in a confined volume. Thus, pyrene is a fascinating core for constructing fluorescent-conjugated

light emitting dendrimers. In addition, several types of chromophoric dendrimers backbone such as polyphenylene (Gong et al., 2001; Xu et al., 2002; Kimura et al., 2001), poly(phenylacetylene) (Xu & Moore, 1993; Meliger et al., 2002), and poly(benzyl ether) (Jiang & Aida, 1997; Harth et al., 2002) have been widely used as light absorbers, and the energy was efficiently funnelled to the core accepter. In this section, we presented the synthesis and photophysical properties of pyrene-cored light-emitting dendrimers that have been investigated for the preparation of optoelectronically active solution-processable light emitting dendritic materials and concentrate on the potential applications in OLEDs, in

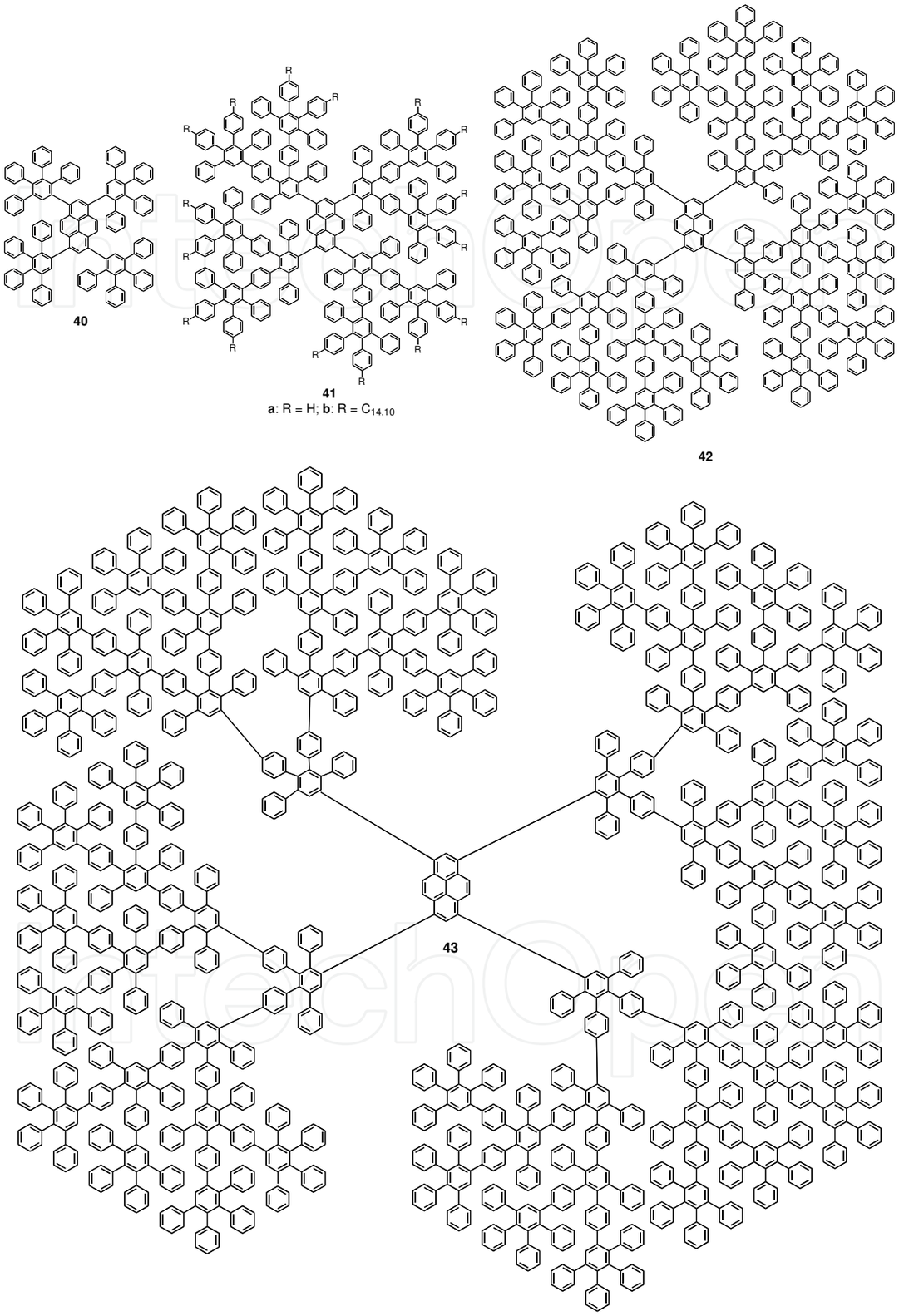


Fig. 6. Polyphenylene-functionalized pyrene-cored light emitting dendrimers (**40**-**43**).

which some light emitting dendrimers have been used. Due to its highly stiff, rigid, and shaped-persistent dendritic backbone (Wind et al., 2001; Rosenfeldt et al., 2003, 2004), recently, Mullen and co-workers (Bernhardt et al., 2006) successfully prepared a series of encapsulation (**40-43**, Figure 6) in a rigid polyphenylene shell using pyrene as chromophore and electrophore core. Around the fluorescent pyrene core, a first-generation (**40**), a second-generation (**41**), a third-generation (**42**), and a fourth-generation (**43**) polyphenylene dendritic environment consisting pyrene building blocks are constructed starting from the fourfold ethynyl-substituted chromophore, 1,3,6,8-tetraethynylpyrene by combining divergent and convergent growth methods. All UV-vis absorption spectra of the first- to fourth-generation dendrimers **40**, **41a**, **42**,and **43** in $CHCl_3$ showed two distinct bands, one in the visible region at ca. 395 nm and the other in the UV region at ca. 280-350 nm. The absorption in the visible region is due to the $\pi$-$\pi^*$ transition of the pyrene core and showed a red shift of up to 55 nm compared with unsubstituted parent pyrene (337 nm). Additionally, the fine structure of the pyrene absorption spectrum was lost due to substitution with the phenyl rings. The absorption band in the UV region can be predominantly attributed to the polyphenylene dendrons (Liu et al., 2003), as indicated by the linear increase in theextinction coefficients $\varepsilon(\lambda)$ with increasing number of attached phenylene moieties. The emission spectra of **40**, **41a**, **42**, and **43** displayed a broad emission band at 425 nm upon excited the pyrene core at 390 nm. No change was observed in emission maximum or fluorescence intensity of the pyrene core with the changes of the dendrimers generation. Excitation of the polyphenylene dendrons at 310 nm resulted in strong emission of the pyrene core at 425 nm, which indicates efficient energy transfer from the polyphenylene dendrons to the pyrene core. By using 9,10-diphenylanthracene as reference chromophore, the fluorenscence quantum yields$\Phi_f$ of **40**, **41a**, **42**, and **43** in $CHCl_3$ were determined at 0.92-0.97. Furthermore, the Stern-Volmer quenching experiments and temperature-dependent fluorescence spectroscopy indicated that a second-generation dendrimers shell (**41**) is sufficient for efficiently shielding the pyrene core and thereby suppressing aggregation. In order to investigate the solid-state photophysics of polyphenylene-dendronized pyrenes (**40-43**), the absorption and emission spectra of alkyl-chain-decorated second-generation dendromers **41b** were recorded. Films of good optical quality were obtained by Simple drop casting and spin coating from toluene solution onto quartz substrates. Thin-film of the second-generation 41b displayed an absorption maximum of at 393 nm, almost unshifted compared with solution spectra. The absorption band in the UV region (ca. 260 nm) should be assigned to the polyphenylene dendrons. The emission spectra of **41b** occurred at 449 nm, that is, a bathochromic shift of only 20 nm compared with solution spectra. Thus, these pyrene-cored dendrimers (**40-43**) are exciting new light-emitting materials that combine excellent optical features and good film-forming ability, which make them promising candidates for several applications in electronic devices such as OLEDs.

The synthesis and characterization of a new class of dendrimers (**44** (PyG0), **45** (PyG1), and **45** (PyG2), Figure 7) consisting of a polysulfurated pyrene core, namely, 1,3,6,8-tetra-(arylthio)pyrene moiety, with appended thiophenylene units, recently, reported by Gingras *et al*. (Gingras et al., 2008). The UV-vis absorption spectra of the compounds **44** (PyG0), **45** (PyG1), and **45** (PyG2) in $CH_2Cl_2$ solutions showed broad absorption band in the visible region with a maximum at 435 nm, which is essentially the identical for the three dendrimers, can be straightforwardly assigned to the pyrene core strongly perturbed by the four sulfur substituents. The band with a maximum around 260 nm can be assigned to the dendrons of thiophenylene units, which increase in intensity with the dendrimers generation. The emission bands for these three dendrimers in $CHCl_3$ solutions

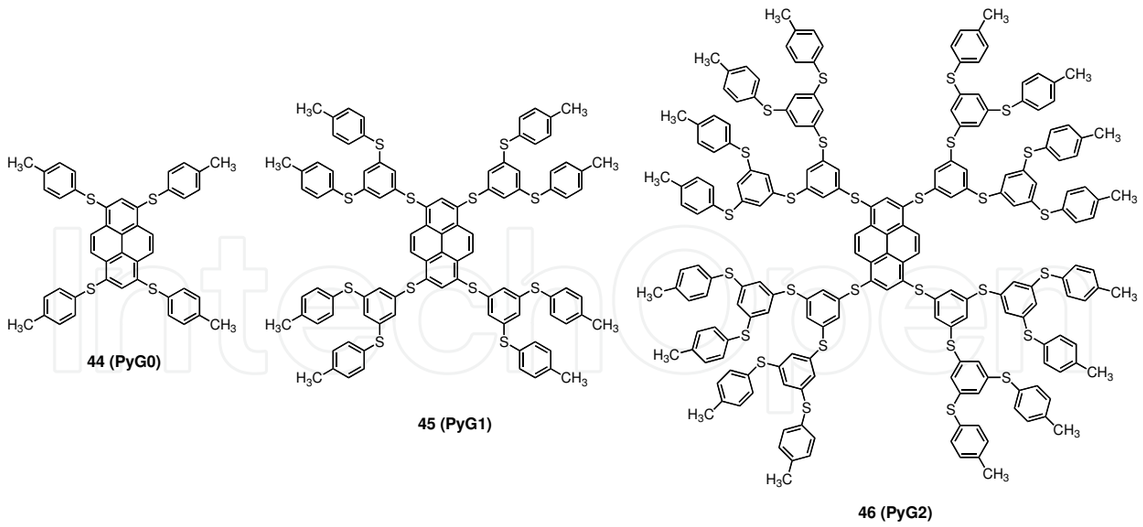


Fig. 7. Polythiophenylene-functionalized pyrene-cored light emitting dendrimers (**44**-**46**).

strongly red-shifted with maximum at 448 nm for **44**, 452 nm for **45**, and 457 nm for **46**, respectively, compared to that of pyrene (375 nm). Compared to pyrene (277 ns), a remarkable difference is that the excited state lifetime is so short at 1.4-2.4 ns that it is unaffected by the presence of oxygen. The strong fluorescence is also present in the solid state (powder) as a broader band at lower energy with the same lifetime. The fluorescence anisotropy and redox properties for the three dendrimers **44-46** were also investigated in cyclohexane solution at 293 K and in $CH_2Cl_2$ solutions, respectively. Thus, these newly developed dendrimers with unique photophysical properties might be exploited for optoelectronic and electrochromic applications.

Examples of light emitting dendrimers including pyrene both at the core and periphery are very rare (Mondrakowski et al., 2001), and multichromophoric dendrimers consisting exclusively of pyrene units have recently been reported by Mullen group (Figueira-Duarte et al., 2008). They designed and characterized a new type of light emitting dendrimers, polypyrene dendrimers, represented by the first-generation dendrimer (**49**, **Py(5)**) and the second-generation dendrimers (**50**, **Py(17)**), consisting of five and seventeen pyrene units, respectively, as well two model compounds, **47** (**Py(2)**), and **48** (**Py(3)**), comprising two and three pyrene chromophores, respectively (Figure 8). The UV-vis absorption and fluorescence spectra of the polypyrene dendrimers **Py(*n*)** (n = 2, 3, 5, and 17) were recorded in toluene at 25 ˚C. In the absorption spectra, from **47 (Py(2)** to **50 (Py(17)**, the broad red sifted from the structural part of the spectrum increases in relative intensity. This broad band reflects the intramolecular interaction between the pyrene units in the **Py(*n*)** compounds, which becomes stronger from **47** to **50**. The fluorescence spectra of **Py(2)** consists of a single band, with some vibrational structure. The fluorescence band shifts to red from 23300 $cm^{-1}$ for **47** (**Py(2)**) to 20660 $cm^{-1}$ for **50** (**Py(17)**), with a simultaneous loss of structure. The fluorescence quantum yields ($\Phi_f$) are 0.72 for **47**, 0.72 for **48**, 0.70 for **49**, and 0.69 for **50**, respectively. The fluorescence decay times of **47** (**Py(2)**), **48** (**Py(3)**), and **49** (**Py(5)**) are 1.76, 1.86, and 1.51 ns, respectively, while, for **50** (**Py(17)**), a triple-exponential decay is found, with $\tau_1$ = 1.75 ns as the major component. The results indicates that the intermolecular excimer formation in the polypyrene dendrimers **47-50** can be excluded due to their small concentrations (< $10^{-5}$ mol $L^{-1}$) and the short monomer-fluorescence lifetime $\tau_1$ of around 2 ns. In addition, the

computed structures (AM1) analysis of **49** (**Py(5)**) and **50** (**Py(17**)) revealed that the calculated dihedral angle between the core and the first branch is 65-66° for **Py(5)** and 71-73° for **Py(17)**, with the angle between the first and the second branch in **Py(17)** around 84-89°. Thus, the rigid and strongly twisted 3D structure allows a precise spatial arrangement in which each unit is a chromophore. Furthermore, the results on photophysical properties and molecular structure design make these dendrimers model compounds or attractive candidates for use as fluorescence labels or optoelectronics applications.

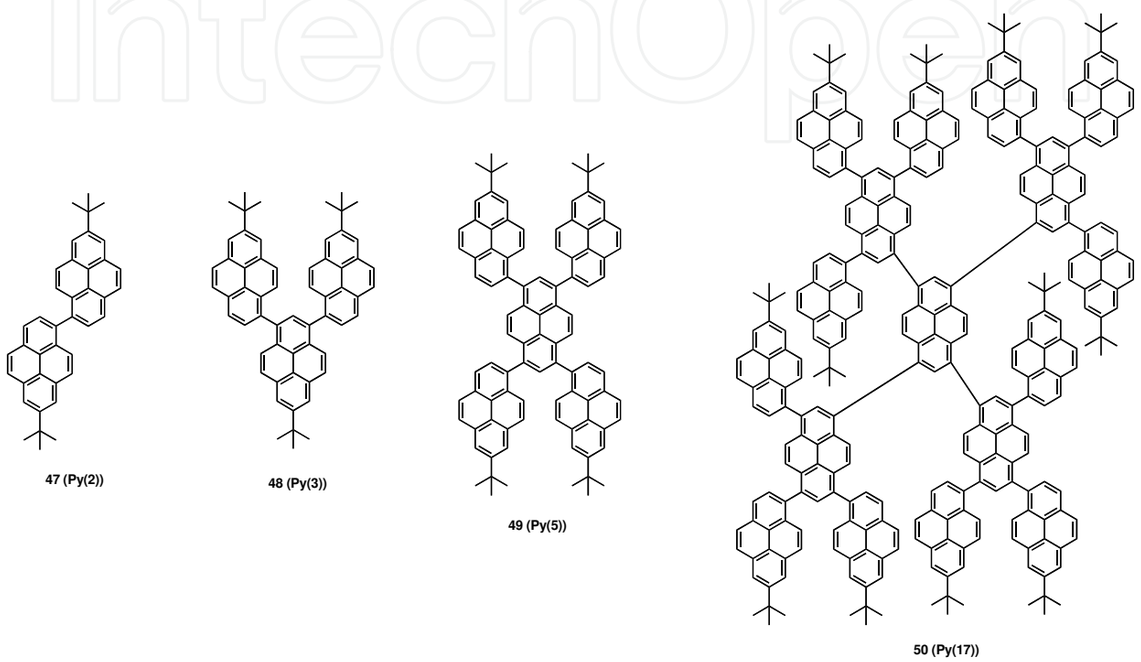


Fig. 8. Polypyrene light emitting dendrimers (**47-50**).

In recent years, one-dimensional self-assembly of functional materials has received considerable interest in the fabrication of nanoscale optoelectronic devices (Lehn, 1995). Research reports (Hill et al., 2004; Kastler et al., 2004; Balakrishnan et al., 2006) suggest that the aromatic organic molecules and large macromolecules are prone to one-dimensional self-assembly through strong π-π interactions. For example, the self-assembly of stiff polyphenylene dendrimers with pentafluorophenyl units has reported by Mullen group (Bauer et al., 2007), in which the driving force for nanofiber formation is attribute to the increase in intermolecular π-π stacking and van der Waals interactions among dendrons by pentafluorophenyl units. On the other hand, for the acetylene-linked dendrimers, their stretched and planar structures may enable facial π-π stacking, resulting in efficient intermolecular electronic coupling. More recently, Lu and co-workers (Zhao et al., 2008) reported two new solution-processable, fluorinated acetylene-linked light emitting dendrimers (**51**a (**TP1**) and **51b** (**TP2**), Figure 9) composed of a pyrene core and carbazole/fluorene dendrons. The strong electron-withdrawing groups of tetrafluorophenyl are introduced at the peripheries of the dendrimers may enhanced electron transportation (Sakamoto et al., 2000), thus balancing the number of holes and electrons in LEDs devices. Both dendrimers are highly soluble in common organic solvents. Their thermal stability is investigated by differential scanning calorimetry (DSC) and thermogravimetric analysis

(TGA) in $N_2$ at a heating rate of 20 ˚C/min. dendrimers **TP1** and **TP2** exhibit high glass-transition temperatures ($T_g$'s) at 142 and 130 ˚C, respectively, and decomposition temperatures ($T_d$'s, corresponding to a 5 % weight loss) at 456 and 444 °C, respectively. The UV-vis absorption spectra of the dendrimers in $CH_2Cl_2$ solutions exhibit two prominent absorption bands: the first band is attributed to the π-π* transition of the core (pyrene with a certain extension) with a maximum peak at ca. 501 nm, which reveals that the dendrimers are highly conjugated; the second bands is should assigned to the dendrions with a maximum peaks at ~390 nm for **TP1** and ~399 nm for **TP2**. In the case of thin neat films, similar absorption spectra for both dendrimers are observed except for a slight red shift and a loss of fine structures. Upon excitations, both dendrimers **TP1** and **TP2** exhibit emission peaks located at 522 nm with a shoulder at ~558 nm, which is attributed to the emission of the core. There is only a trace emission from the dendrons in the range of 400~450 nm, which indicates efficient photon harvesting and energy transfer from dendrons to the core.

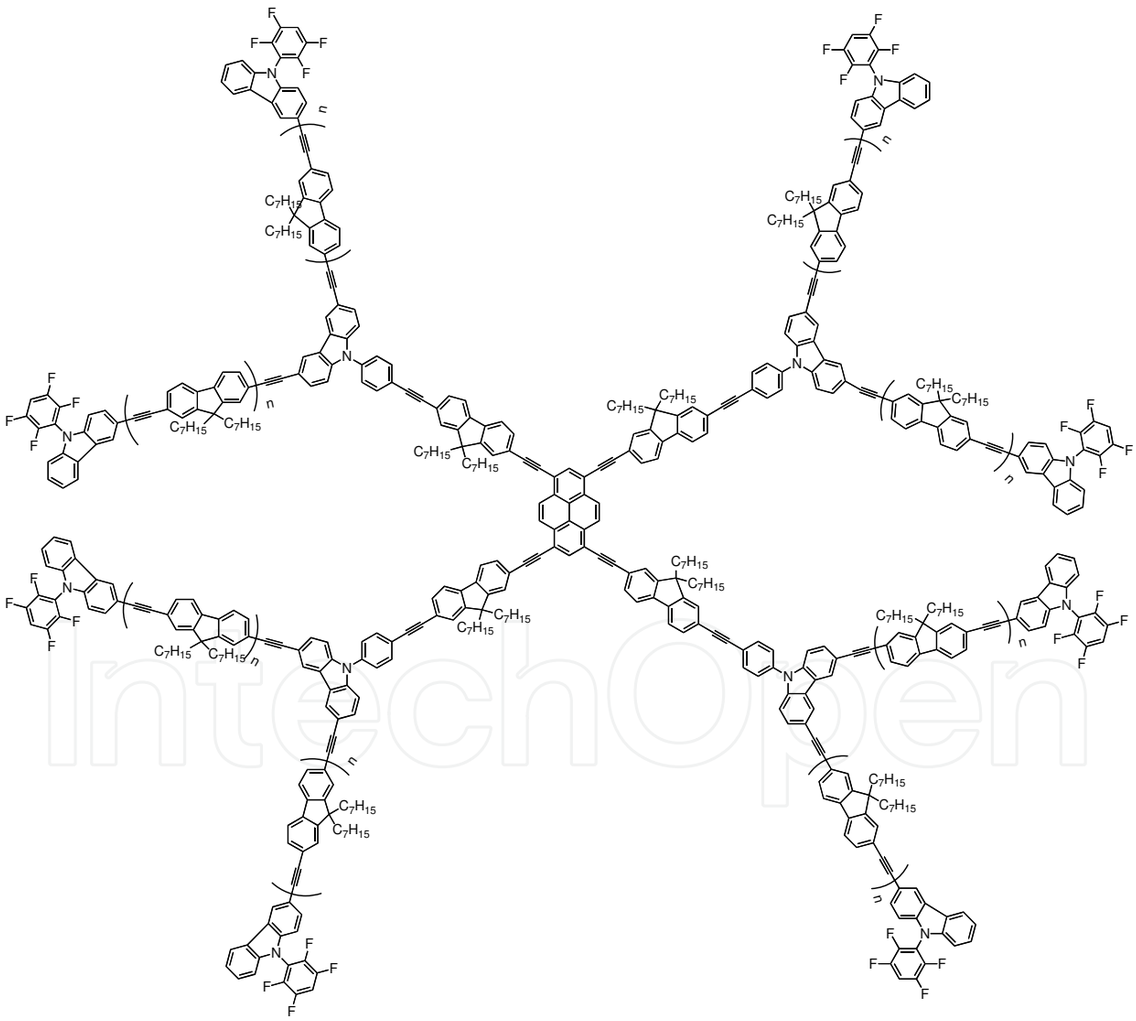

**51 a:** n = 1 (TP1)
**b:** n = 2 (TP2)

Fig. 9. Fluorinated acetylene-linked pyrene-cored light emitting dendrimers (**51**).

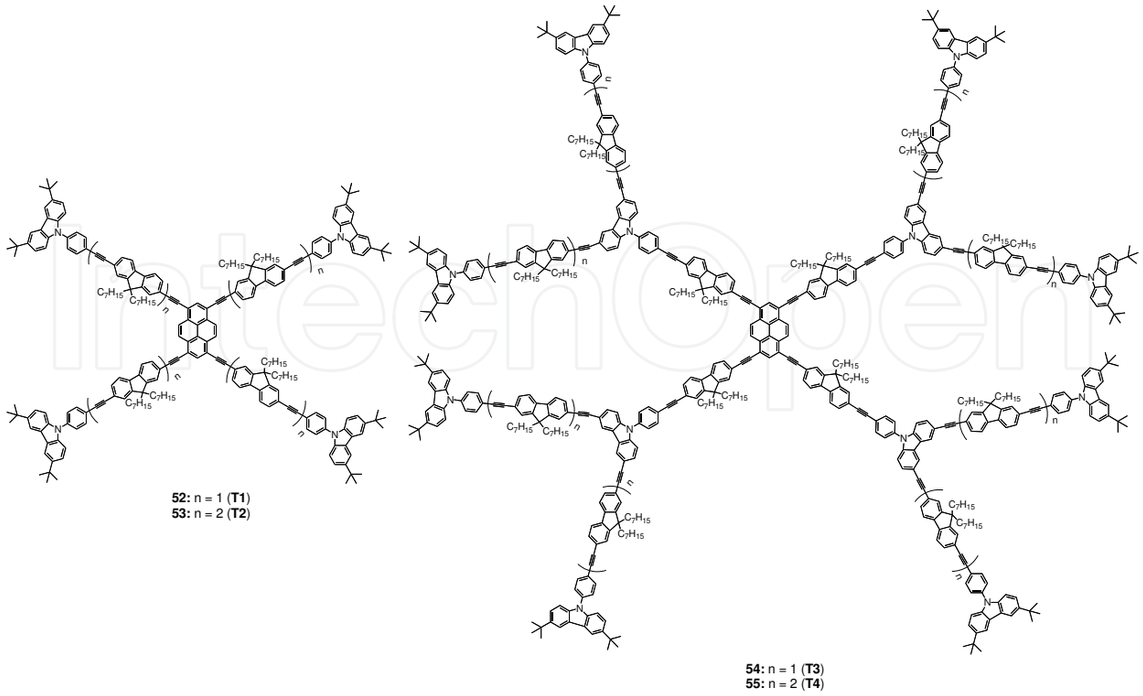


Fig. 10. Aacetylene-linked pyrene-cored light emitting dendrimers (**52**-**56**, **T1**-**T5**).

In the thin films, **TP1** and **TP2** exhibit strong yellow emission with peaks at 532 nm and 530 nm and relatively peak at 568 nm, respectively, which are ascribed to aggregate formation in the solid states. A nanofibrous suspension was obtained in $CH_2Cl_2$ solution of **TP1** due to its facile one-dimensional self-assembly property. Interestingly, the nanofiber suspension exhibits a green emission with a peak at 498 nm, which is blue-shifted by 34 nm with respective to that of thin neat film. This blue-shifted emission is somewhat abnormal because, generally, aggregations of molecules through intermolecular π-π interaction should result in a red-shifted emission (Balakrishnan et al., 2005; Hoeben et al., 2005). Thus, these finding suggests that the self-assembly process occurs in a nonhomocentric way. Atomic force microscopy (AFM) detected that compounds **TP1** and **TP2** exhibited good film-forming ability despite its rigid and hyperbranched structures. The EL properties of **TP1** and **TP2** were fabricated with the configuration of ITO/PEDOT (25 nm)/**TP1** or **TP2**/$Cs_2CO_3$ (1 nm)/Al (100 nm) by spin-coating with 1500 rpm from their 2% (wt%) *p*-xylene solutions. Two dendrimers exhibit yellowish green with main peaks at 532 nm and shoulder peaks at 568 nm and CIE coordinates of (0.38, 0.61) for **TP1** and (0.36, 0.62) for **TP2**, respectively. The devices exhibits a maximum efficiency of 2.7 cd/A at 5.8 V for **TP2**, 1.2 cd/A at 6.4 V for **TP1**, and a maximum brightness of 5300 cd/m² at 11 V for **TP2**, 2530 cd/m² at 9 V for **TP1**, respectively. These obtained results indicated that the dendrimers with fluorinated terminal groups are promising candidates for optoelectronic materials. Quite recently, Lu and co-workers (Zhao et al., 2009) reported another series of acetylene-linked,solution-processable stiff dendrimers (**52-56**, **T1-T5**, Figure 10) consisting of a pyrene core, fluorene/carbazole-composed dendrons. The dendrimers **52-56** show good thermal stability, strong fluorescence, efficient photo-harvesting, and excellent film-forming properties. The single-layer devices with a configuration of ITO (120 nm)/PEDOT (25 nm/**dedrimer**/$Cs_2CO_3$ (1 nm)/Al (100 nm) are fabricated and fully investigated. The dendrimer films are fabricated

by a spin-coating speed ranging from 800 to 3500 rpm from their *p*-xylene solutions. For example, at a speed of 1500 rpm, the **T3**-based LED exhibits yellow EL (CIE: 0.49, 0.50) with a maximum brightness of 5590 cd/m$^2$ at 16 V, a high current efficiency of 2.67 cd/A at 8.6 V, and a best external quantum efficiency of 0.86%. These results indicate the constructive one offsets the distinctive effect of intermolecular interaction.

## 5. Functionalized pyrene-based light-emitting oligomers and polymers

In recent years, organic materials with π-conjugated systems, such as conjugated polymers (Kraft et al., 1998) and monodisperse conjugated oligomers (Mullen & Wenger, 1998) have been intensively studied due to their potential applications in photonics and optoelectonics, such as field-effect transistors (FETs) (Tsumura et al., 1986), OLEDs (Burroughes et al., 1990), solar cells (Brabec et al., 2001), and solid-state laser (McGehee & Heeger, 2000), and the academic interest on the structure-property relationship of molecules. To date, many π-conjugated oligomers and polymers possessing benzene, naphthalene, thiophene, and porphyrin as a conventional core. Although pyrene is a fascinating core in fluorescent π-conjugated light-emitting monomers and dendrimers, the use of pyrene as central core for the construction of oligomers or polymers is quite race.

Purified by precipitated, conjugated polymers are typically characterized by chemical composition and distribution in chain length. However, the polydispersity in chain length leads to complex structural characteristics of the thin films, and make it very difficult for researchers to establish a proper structure-property relationship. In contrast, monodisperse conjugated oligomers are strucrally uniform with superior chemical purity accomplished by recrystallization and column chromatography. Thus, oligomers generally possess more predictable and reproducible properties, facilitating systematic investigation of structure-property relationship and optimization. Recently, some pyrene-based conjugated light-emitting oligomers and polymers have been reported. For instance, pyrene-cored crystalline oligopyrene nanowires (**57**, Figure 11) exhibiting multi-colored emission have been reported by Shi *et al*. (Qu & Shi, 2004). Inoue and co-workers reported the synthesis and photophysical properties of two types of acetylene-linked π-conjugated oligomers based on alkynylpyrene skeletons (Shimizu et al., 2007). The chemical structures of these alkynylpyrene oligomers **58** and **59** are also show in Figure 11, and the structural difference between **58** and **59** is only the linkage position of terminal acetylene groups on the benzene rings, i.e., *para* for **58** and *meta* for **59**. The optical properties of the oligomers **58** and **59** were investigated by using $CHCl_3$ as a solvent at dilute concentrations ($1.0 \times 10^{-6}$ M) under degassed conditions, respectively. Both absorption maximum and its corresponding coefficient (log ε) of the *para*-linked oligomers **58** are varied from 436 nm to 454 nm, and 4.84 $M^{-1}$ $cm^{-1}$ to 5.58 $M^{-1}$ $cm^{-1}$, with increasing of oligomer length. In the case of *meta*-linked oligomers **59** only a slight bathochromic shift was observed that varied from 440 nm to 444 nm with increasing of oligomer length, which probably because of partial insulation of the π-conjugation on these oligomers. The fluorescence spectra of the oligomers were also measured in degassed $CHCl_3$ solutions. Two strong emission bands were observed in the visible region in all spectra. The emission maxima for the *para*-linked oligomers **58** shifted to longer wavelength from 448 nm to 473 nm, in a manner similar to their absorption maximum. On the other hand, for the *meta*-linked oligomers **59**, the fluorescence spectra varied from 455 nm to 461 nm in agreement with the electronic absorption spectra. The fluorescence quantum yields ($\Phi$) were found in the range of 0.35-0.74 in $CHCl_3$ and 0.44-0.79

in THF, respectively. Thus, the newly developed π-conjugated oligomers will facilitate the synthesis of alkynylpyrene polymers and the useful to optical devices.

More recently, Lu and co-workers reported (Zhao et al., 2007) a series of highly fluorescent, pyrene-modified light-emitting oligomers, namely, pyrene-end-capped oligo(2,7-fluorene ethynylenes)s (**60-62**) and pyrene-centered oligo(2,7-fluorene ethynylenes)s (**63-65**) (Figure 11). The absorption spectra of the oligomers were investigated in both dilute $CH_2Cl_2$ solutions and in thin neat films. For the pyrene-end-capped oligomers **60**, **61**, and **62**,

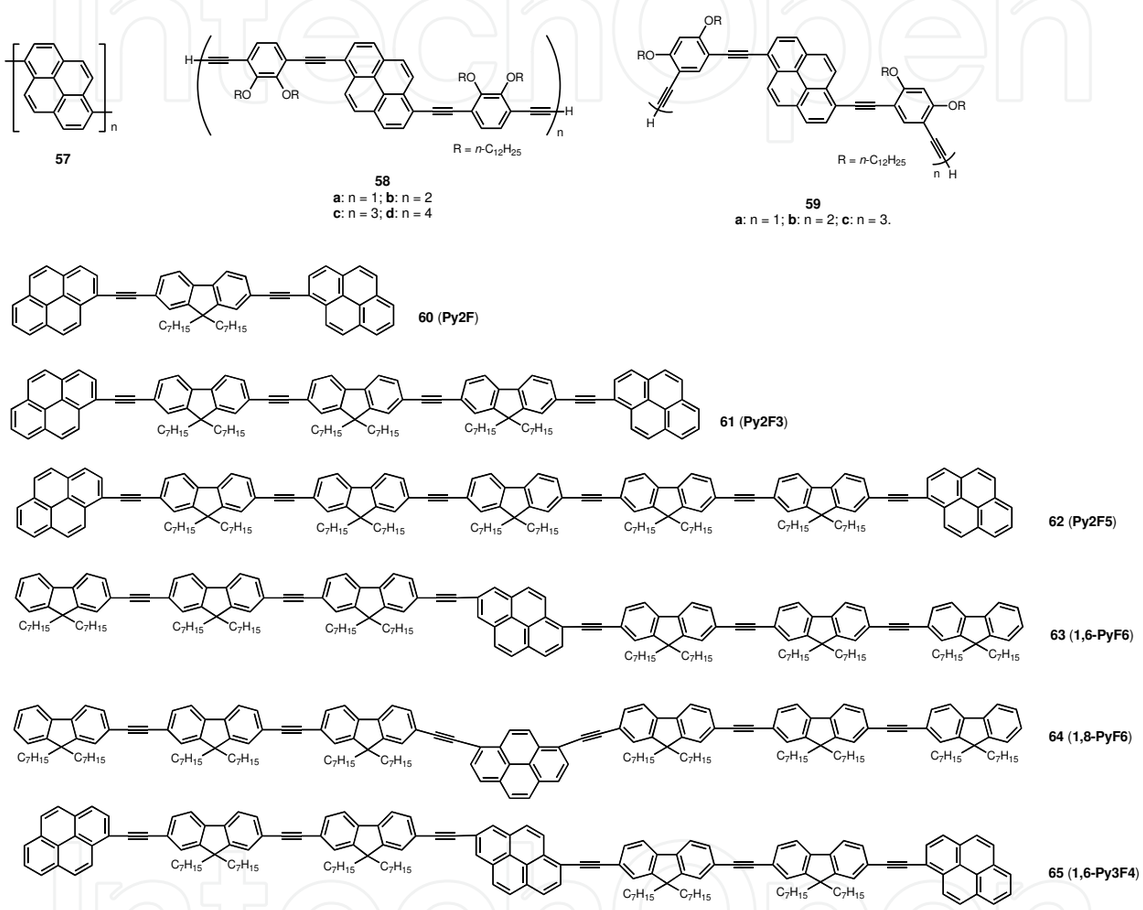


Fig. 11. Functionalized pyrene-based light-emitting oligomers (**57**-**65**).

the maximum absorption peaks were located at 426, 421, and 418 nm, respectively, which could be attributed to the π-π* transition of the molecular backbone. A interesting blue-shift was observed as the molecular chain length increased, which might be due to the complicated intramolecular conformation such as the two pyrene units might not conjugate to the whole molecular backbone efficiently at one time, thus lead to a weak influence. Compared to that of pyrene-end-capped oligomer **Py2F5** (**62**), the pyrene-centered 1,6-PyF6 (**63**) and 1,6-Py3F4 (**65**) show red-shifted by ~33 nm located at ~451 nm. 1,8-PyF6 (**64**) exhibited a similar maximum absorption peak in comparison to that of 1,6-PyF6, but the relative absorption intensity changed, which might be due to the interruption of delocalization of the π-electrons along the oligomer backbone by the 1,8-pyrene linkage. All absorption spectra in solid-state for these oligomers were almost identical, but had a slightly

bathochromic shift (2-10 nm) compared to the corresponding solutions, which indicated that these oligomers exhibited very similar conformations in both states (Chen et al., 2005). In $CH_2Cl_2$ solutions, the PL spectra of the pyrene-end-capped oligomers **60**, **61**, and **62** showed a main emission peak at 436, 430, and 429 nm, respectively, with a shoulder peak at 464, 456, and 455 nm, respectively. The blue-shift emissions were attributed to the same reason for blue-shifted absorption spectra of them. On the other hand, the PL spectra of the pyrene-centered oligomers 63-65 exhibited quite similar main emission peaks at ~465 nm with shoulder peaks at ~495 nm, actually emanating from disubstituted pyrene. In thin neat films, the disappearance of the fine structures of spectra were observed with main peaks at 492 nm for **60**, 489 nm for **61**, and 476 nm for **62**, respectively. Emission of Py2F (**60**) was strongly red-shifted by 56 nm compared to the emission in solution which should be due to the facile formation of excimers between pyrene units. All the oligomers were highly fluorescent. The PL quantum yields of these oligomers were in the range of 0.78-0.98 in degassed cyclohexane solutions using 9,10-diphenylanthracence (DPA, $\Phi$ = 0.95) as a standard (Melhuish, 1961). Moreover, Py2F5 (**62**) exhibitedhigher quantum yields than the pyrene-centered oligomers **63-65** with similar chain length, which might be that excitons were well confined to the whole backbone of Py2F5 (**62**). By using these oligomers as emitters, the devices with the same configurations of ITO/PEDOT: PSS (30 nm)/ **oligomers** (50 nm)/TPBI (20 nm)/Al (100 nm) were fabricated. For the pyrene-end-capped oligomers **60-62**, the EL emissions were observed from green (532 nm) to blue (468 nm) with the increment of the fluorene moieties. The EL emission of **60** (Py2F) was significantly red-shifted (40 nm) comparison with that of PL emission in film, while the EL emission of **62** (Py2F5) was slightly blue-shifted (8 nm). Since **60** (Py2F) had the shortest chain length among the pyrene-end-capped oligomers, the highest chain mobility was suggested. Results have pointed out that materials with repeating fluorene units should be underwent a process of alignment in an electric field, and molecules with the high chain mobility more easily formed excimers than molecules with low chain mobility (Weinfurtner et al., 2000). Due to the higher chain mobility of **60** compared to that of **61** and **62**, it is was more possible for **60** molecules to align under the electric field. Thus, the pyrene groups on one Py2F (**60**) molecule could be close to the pyrene groups on the neighbouring molecules, and when the distance between the two fluorophores was appropriate, excimers were formed under the electric excitations. On the other hand, for the pyrene centered oligomers **63-65**, the EL spectra showed green emissions from 472 to 504 nm, which similar to their corresponding PL emission in films except for slight red shifts. The results indicate that both PL and EL emission originated from the same radiative decay process of singlet excitons. The turn-on voltages of the oligomers-based devices were in the range of 4.3-5.4 V. the **Py2F**-based device exhibited maximum brightness at 2869 cd/cm$^2$ at 10.5 V and a highest external quantum efficiency of 0.64%. While with the increase of the fluorene moiety, the device based on **Py2F3** and **Py2F5** exhibited a substantial decrease of maximum brightness from 918 cd/cm$^2$ at 9.0 V to 207 cd/cm$^2$ at 8.0 V as well as the external quantum efficiency of 0.41% for **Py2F3** and 0.15% for **Py2F5**. The pyrene-end-capped-based devices exhibited comparable brightness, 493 cd/cm$^2$ at 8.5 V for **63**, 520 cd/cm$^2$ at 8.5 V for **64**, and 340 cd/cm$^2$ at 6.5 V for **65**, respectively, as well as an external quantum efficiency, 0.22% (**63**), 0.22% (**64**) and 0.14% (**65**), respectively. Obviously, as chain length elongated, the performance of the devices was decreased. One possible explanation for this phenomenon was that the oligomrs with more fluorene moieties were more easily crystallized than the

oligomers with fewer fluorene units. It was well known that crystallization was disadvantageous to the electroluminescence properties of organic materials. As a result, the good performance of the pyrene-modified oligomers-based devices indicated that they were promising light-emitting materials for efficient OLEDs.

In comparison of small molecules, conjugated polymers have the advantageous of being applicable in larger display sizes and lighting devices at much lower manufacturing costs via solution-based deposition techniques. Conjugated polymers such as polyphenylvinylene (PPV) and its derivatives are known as visible light emitters and have been widely used in the fabrication of organic light-emitting diodes (OLEDs) (Son et al., 1995). Only a few numbers of investigations concerning on the attachment of pyrene to the polymeric chain (Rivera et al., 2002) or the use of pyrene along the polymeric backbone (Ohshita et al., 2003; Mikroyannidis et al., 2005; Kawano et al., 2008; Figueira-Duarte et al., 2010) were reported as model systems or new materials for molecular electronics.

Giasson and co-workers reported (Rivera et al., 2002) the synthesis and photoproperties of four different polymers (**66** (**PEP**), **67** (**PTMSEP**), **68** (**PBDP**), and **69** (**PTMSBDP**), Figure 12) by the W and Ta-catalyzed polymerization of 1-ethynylpyrene, 1-(trimethylsilylethynyl)-pyrene, 1-(buta-1,3-diynyl)pyrene, and 1-(4-trimethylsilylethynyl)pyrene, respectively, in which pyrene as functional group attached in the polymeric chain. For comparison, the dimmer of 1-ethynylpyrene (**DEP**) was prepared. The absorption spectra of the polymers and **DEP** are recorded in THF. For **DEP**, three peaks were observed, the peak at 336 nm can be attributed to the pyrene moieties, and the peak at 346 nm and shoulder peak at 390 nm should have their origin in intramolecular interactions (complexation) between the pyrene units present in the dimer. The absorption spectrum of **PEP** is significantly different from that of **DEP**. The shoulder peak around 390 nm in **DEP** disappeared in the absorption spectra of **PEP**. This suggests that the intramolecular interactions between adjacent pyrene units in the polymer are weaker than those in **DEP**. Moreover, a broad band is observed around 580 nm in the absorption of **PEP**, which should be caused by the polyacetylene chain. The result indicates that the effective electronic conjugation is relatively long for this polymer. The absorption spectra of **PTMSEP**, **PBDP**, and **PTMSBDP** are relatively similar to each other. However, the bands of **PTMSBDP** and **PBDP** are broader than that of **PTMSEP** suggesting that stronger interactions between pyrene units are present in the former polymers. Thus, two facts can be demonstrated that the distortion of the polymer backbone caused by the presence of a trimethylsilyl group significantly weakens the electronic interactions between pyrene moieties and the incorporation of triple bond into the polymeric chain permits better interactions between the pyrene units. On the other hand, the band around 580 nm observed in **PEP** is not observed for these polymers, which indicates that the effective conjugation is much shorter. In the fluorescence spectra of **DEP** and **PEP** in THF, both compounds show a band in the range of 360-465 nm arising from non-associated pyrene moieties. **DEP** also shows a broad band around 480 nm, which should due to the molecular interactions between pyrene units present in this molecule. Surprisingly, such a distinct band is not observed in the case of PEP that might be caused by an inner-filter effect involving the main chain. However, the fluorescence intensity of **PEP** near 480 nm is significant. This strongly suggests that a complex between pyrene units is also formed in the polymer. The fluorescence spectra of **PTMSBDP** and **PBDP** show two distinct bands similar to the ones observed in the fluorescence spectra of **DEP**. These results are consistent with the absorption spectra of these two polymers showing that strong interactions exist between pyrene moieties in the conjugated chain. However, the

fluorescence intensity around 480 nm is much reduced in the case of **PTMSEP**, further confirming the above results that the incorporation of trimethylsilyl groups into the polymeric backbone decreases the interactions between the pyrene units. On the other hand, the band around 580 nm observed in **PEP** is not observed for these polymers, which indicates that the effective conjugation is much shorter. In the fluorescence spectra of **DEP** and **PEP** in THF, both compounds show a band in the range of 360-465 nm arising from non-associated pyrene moieties. **DEP** also shows a broad band around 480 nm, which should due to the molecular interactions between pyrene units present in this molecule. Surprisingly, such a distinct band is not observed in the case of PEP that might be caused by an inner-filter effect involving the main chain. However, the fluorescence intensity of **PEP** near 480 nm is significant. This strongly suggests that a complex between pyrene units is also formed in the polymer. The fluorescence spectra of **PTMSBDP** and **PBDP** show two distinct bands similar to the ones observed in the fluorescence spectra of **DEP**. These results are consistent with the absorption spectra of these two polymers showing that strong interactions exist between pyrene moieties in the conjugated chain. However, the fluorescence intensity around 480 nm is much reduced in the case of **PTMSEP**, further confirming the above results that the incorporation of trimethylsilyl groups into the polymeric backbone decreases the interactions between pyrene units. On the other hand, by using pyrene as the polymeric backbone, pyrene-based polymers have been studied by several research groups. For example, Ohshita *et al*. prepared (Ohshita et al., 2003) two organosilanylene-diethynylpyrene polymers **70** and **71** (Figure 12) by the reactions of 1,6-di(lithioethynyl)pyrene and the corresponding dichloroorganosilanes. The hole-transporting properties of the polymers were evaluated by the performance of electroluminescent (EL) devices with the configuration of ITO/polymer **70** or **71** (70-80 nm)/$Alq_3$ (60 nm)/Mg-Ag, in comparison with those of an organosilanylene-9,10-diethynyl-anthracene alternating polymer, reported previously (Adachi et al., 1997; Manhart et al., 1999). Among them, the device with polymer **70** (device I) exhibited the best performance with a maximum luminescence of 6000 cd/cm$^2$. This is presumably due to the favored inter- and intra-molecular π-π interactions in the solid states by reducing the volume of the

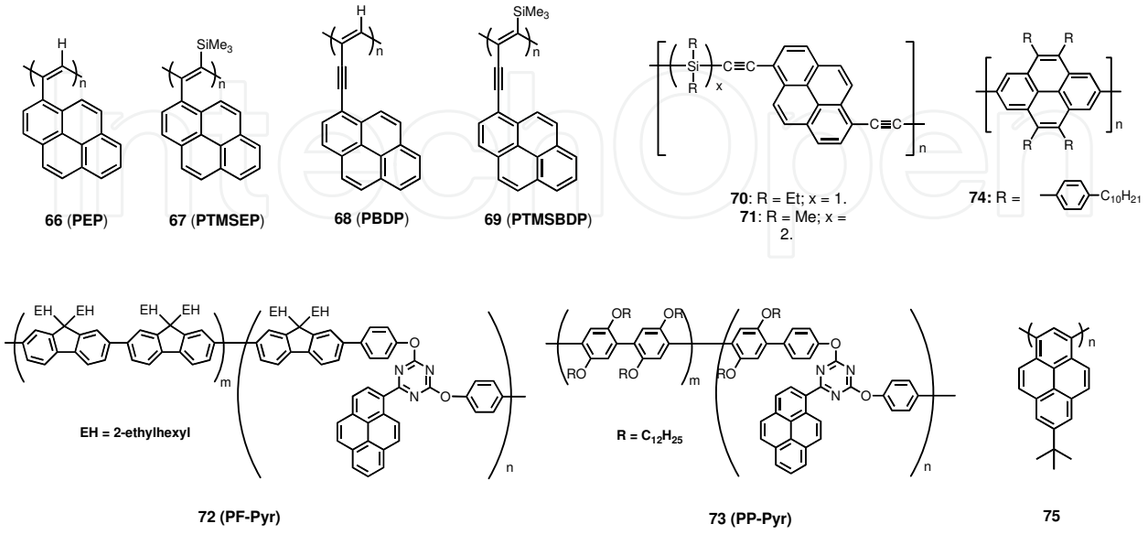


Fig. 12. Functionalized pyrene-based light-emitting polymers (**66**-**69** and **70**-**75**).

silicon units. Further improvement of the performance of the device with polymer **70** was realized by introducing a TPD (*N,N'*-diphenyl-*N,N'*-di(*m*-tolyl)-1,1-biphenyl-4,4'-diamine) layer as electron-block with the structure of ITO/**70** (40 nm)/TPD (10 nm)/$Alq_3$ (60 nm)/Mg-Ag (device II). The optimized device emitted a maximum brightness of 16000 cd/cm$^2$ at the bias voltage of 14-16 V. when compared with that of the device of ITO/**TPD** (50 nm)/$Alq_3$ (60 nm)/Mg-Ag (device III), the device II showed lower turn-on voltage (4-5 V for device II and 6 V for device III) and higher current density. These results clearly indicate the excellent hole-transporting properties of polymer **70** films. Mikroyannidis and co-workers recently reported (Mikroyannidis et al., 2005) the synthesis, characterization and optical properties of two new series of soluble random copolymer **72** (**PF-Pyr**) and **73** (**PP-Pyr**) (Figure 12) that contain pyrenyltriazine moieties along the main chain by Suzuki coupling. The photophysical properties of these polymers were fully investigated in both solutions and thin films. For the copolymer **PF-Pyr** (**72**), blue emissions in solutions with PL maximum at 414-444 nm (PL quantum yields 0.42-0.56) and green emissions in the thin films with PL maximum around 520 nm were observed, respectively. The green emission in solid state of these random copolymers **72** was a result of the energy transfer from the fluorene to the pyrenyltriazine moieties. For the copolymer **PP-Pyr** (**73**), blue light both in solution and in thin film with PL maximum at 385-450 nm were observed, respectively. More specially, the copolymers **PF-Pyr** (**73**) showed outstanding color stability since their PL trace in thin film remained unchanged with respect to the PL maximum and the spectrum pattern even following annealing at 130 ˚C for 60 h. The color stability of the polymer **PF-Pyr** is an attractive feature regarding the high temperature developed during the device operation.

More recently, Mullen group described (Kawano et al., 2008) the synthesis and photophysical properties of the first 2,7-linked conjugated polypyrenlene, **74** (Figure 12), tethering four aryl groups by Yamamoto polycondensation (Yamamoto, 2003). Although composed of large π-units, the polymer **74** is readily soluble in common organic solvent due to the unique substitution with bulky alkylaryl groups at the 4-, 5, 9-, and 10-positions in pyrene ring. The polymer **74** shows a blue fluorescence emission with a maximum band at 429 nm in solution, fulfilling the requirements for a blue-emitting organic semiconductor. However, the fluorescence spectra of **74** exhibit a remarkable long-wavelength tailing as well as additional emission bands with maximum at 493 and 530 nm. To recognize and verify the most probable explanation for the substantially red-shifted band in the case of **74**, concentration dependence of the fluorescence, solvatochromic shifts of the emission maximum (Jurczok et al., 2000; Fogel et al., 2007), and time-resolved measurements of the fluorescence are investigated. These facts together indicated that the red-shifted broad emission bands are not caused by aggregation, but by intramolecular energy redistribution between the vibrational manifold of the single polymer chain (VandenBout et al., 1997; Becker et al., 2006). Furthermore, the additional red-shifted emission (green color) of the polymer **74** in the solid state could be strongly reduced by blending with a non-conjugated polymer such as the polystyrene. Thus, these properties of the polymer **74** could have application in materials processing, for example, as a surrounding media sensor or optoelectronics.

Quite recently, Mullen research group reported (Figueira-Duarte et al., 2010) the suppression of aggregation in polypyrene **75** (Figure 12) with a highly twisted structure of the polymeric chain. The use of *tert*-butyl groups was crucial for selectively affording substitution at the 1,3-positions in the monomer synthesis, and also for both attaining sufficient solubility and avoiding the use of long alkyl chains. The UV-vis absorption and

PL spectra of the polypyrene **75** exhibit very similar spectra in the diluted THF solution and the thin film. The absorption spectra show a π-π* transition at ca. 357 nm and a higher energy absorption band at ca. 280 nm. In contrast, the emission in both solution and thin film showed a broad unstructured band with a maximum at 441 nm in solution and a slight bathochromic shift to 454 nm in the solid state, respectively. Both a classical concentration dependence analysis (in toluene at different concentration ranging from 0.1 to 1000 mg/L) and the calculated molecular structure of a linear 1,3-pentamer model compound (AM1) for the polypyrene **75** provided good evidence for the absence of excimer and aggregation emission. It is well known that the morphological stability at high temperature is a critical point for device performance. Thermal characterization of the polypyrene **75** was made using differential scanning calorimetry (DSC) and thermogravimetric analysis (TGA), and the influence of thermal treatment on its optical properties was investigated. The high morphological stability and glass transition temperature, $T_g$, could be attributed to the presence of the rigid pyrene unit in the main chain of the polymer. Thus, the device with structure of ITO/PEDOT: PSS/polypyrene **75**/ CsF/Al was fabricated. The device showed bright blue-turquoise electroluminescence with a maximum at 465 nm and a profile very similar to the PL in the solid state. Brightness values at 300 cd/m$^2$ were obtained at 8 V with CIE coordinates of (0.15, 0.32). The devices show remarkable spectral stability over time with only minor changes in the spectra as a consequence of a thermal annealing under device operation. The OLEDs display a detectable onset of electroluminescence at approximately 3.5 V and maximum efficiencies of ca. 0.3 cd/A. The performance of the presented devices is comparable to devices fabricated without evaporated transport layers from similar poly(*para*-phenylene)-type based materials with respect to the overall devices efficiency and brightness (Pogantsch et al., 2002; Jacob et al., 2004; Tu et al., 2004). Thus, the simple chemical route and the exciting optical features render this polypyrene a promising material toward high-performance polymer blue light-emitting diodes.

## 6. Pyrene-based cruciform-shaped π-conjugated blue light-emitting architectures: promising potential electroluminescent materials

In recent years, carbon-rich organic compounds with a high degree of π-conjugation have attracted much attention due to their unique properties as ideal materials for modern electronic and photonic applications, such as organic light-emitting diodes (OLEDs), liquid-crystal displays, thin-film transistors, solar cells and optical storage devices (Meijere, 1998, 1999; Haley & Tykwinski, 2006; Mullen & Weger, 1998; Mullen & Scherf, 2006; Kang et al., 2006; Seminario, 2005; Van der Auweraer & De Schryer 2004). Among them, functionalized, cruciform-shaped, conjugated fluorophores are well-known because they exhibit interesting optoelectronic properties due to their special, multi-conjugated-pathway structures. Examples of cruciform-shaped phores are the 1,2,4,5-tetrasubstituted(phenylethynyl) benzenes of Haley *et al*. (Marsden et al., 2005), the X-shaped 1,2,4,5-tetravinyl-benzenes of Marks *et al*. (Hu et al., 2004), the 1,4-bis(arylethynyl)-2,5-distyrylbenzenes of Bunz *et al*. (Wilson & Bunz, 2005), and other cross-shaped fluorophores developed by Nuckolls *et al*. (Miao et al., 2006) and Scherf *et al*. (Zen et al., 2006). Therefore, their seminal studies on the structure-property relationships for those materials provided valuable information for the molecular design of material as model systems or promising candidates toward high-performance optoelectronic devices.

Accordingly, our previous report (Yamato et al., 1993; Yamato et al., 1997) on the synthesis of 4,5,9,10-tetrabromo-2,7-di-*tert*-butylpyrene prompted us to explore 4,5,9,10-tetrakis(phenylethynyl)pyrenes as emissive materials. We surmised that i) The presence of the sterically bulky *t*Bu groups in pyrene rings at the 2- and 7-positions would play important roles for both inhibiting undesirable face-to-face π stacking in solution and the solid state (Bennistom et al., 2007) and attaining sufficient solubility; ii) The ready synthetic accessibility by the Sonogashira coupling, the phenylacetylenicgroups were a priori anticipated to facilitate the construction of the cruciform-shaped structure and further extend the conjugation length of the pyrene chromophore, resulting in a shift of the wavelength of absorption and fluorescence emission into the visible region of the electromagnetic spectrum. Along this lines, as our efforts on the construction of extended π-conjugation compounds based on pyrene (Hu et al., 2009; Hu et al., 2010), we recently succeed to prepare a new series of pyrene-based, cruciform-shaped, π-conjugated, blue-light-emitting monomers (**79**) with a low degree of aggregations in the solid state and pure-blue emission by various spectroscopic techniques (Hu et al., 2010).

The simple chemical route to the cruciform-shaped conjugated pyrenes **79** is shown in scheme 2. The Lewis-acid-catalyzed bromination of 2,7-di-*tert*-butylpyrene (**76**) (Yamato et al., 1993; Yamato et al., 1997) readily afforded the 4,5,9,10-tetrabromo-2,7-di-*tert*-butylpyrene **77** in high yiled of 90%. The modified Sonogashira coupling of the tetrabromide **77** with various phenylacetylenes **78** produced the corresponding 2,7-di-*tert*-butyl-4,5,9,10-tetrakis(*p*-R-phenylethynyl0pyrenes **79** in excellent yields. As a comparison, 1,3,6,8-tetrakis(4-methoxyphenylethynyl)pyrene **80** is prepared according to literature procedure (Venkataramana & Sankararaman, 2005). The chemical structures of these new pyrenes **79** and **80** were fully confirmed by their $^{1}H/^{13}C$ NMR spectra, FT-IR spectroscopy, mass spectroscopy as well as elemental analysis. All results were consistent with the proposed cruciform-shaped structures.

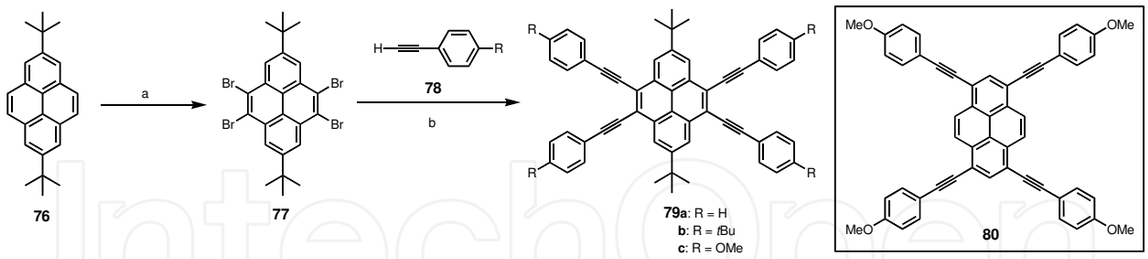


Scheme 2. Synthesis of 4,5,9,10-tetraksi(phenylethynyl)pyrene derivatives **79a-c**. Reagents and conditions: (a) $Br_2$, Fe powder, $CH_2Cl_2$, r. t., for 4 h, 90%; (b) [$PdCl_2(PPh_3)_2$], CuI, $PPh_3$, $Et_3$/DMF (1:1), 24-48 h, 100 °C.

The performance of the organic compounds in optoelectronic devices strongly relies on the intermolecular order in the active layer. Small single crystals of **79c** are suitable for X-ray structural determination under the synchrotron. Both the X-ray crystal-structures diagram and packing diagram of **79c** are shown in Figure 13, respectively. As revealed from this analysis, there is a herringbone pattern between stacked columns, but the π-π stacking average distance of adjacent pyrene units was not especially short at ca. 5.82 Å in this crystal lattice. The results strongly indicate that the two bulky *t*Bu groups attached to the pyrene rings at the 2- and 7-positions play an important role in suppressing the aggregations

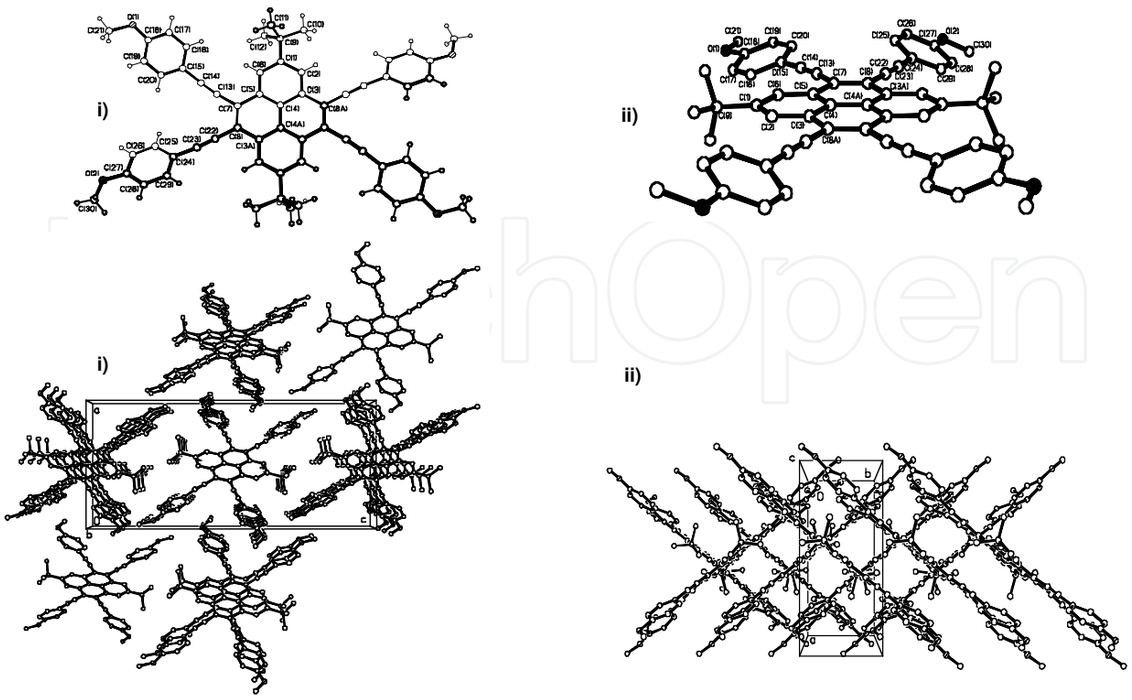


Fig. 13. X-ray crystal-structure diagram of **79c** (i) top view; (ii) side view. down); Packing diagram of **79c** (i) view parallel to *b*, highlighting the π-π stacking; (ii) view parallel to *c*, showing the herringbone packing motif.

in the solid state. Hence, the newly developed cruciform-shaped pyrenes with both the unique intermolecular order of stacked column and low degree of π stacking suggest that they might be advantageous to high charge-carrier transport and robust blue-light emitting materials in optoelectronic devices (Naraso et al., 2005; Wu et al., 2007; Gao et al., 2008).

The UV-vis absorption spectra of **79** are shown in Figure 14, that together with those of pyrenes **76** and **80**. Compared with that of pyrene **76**, the absorption spectra of both **79** and **80** were broad and less well-resolved, and the longest-wavelength, π-π* transition absorption maximum of **79** and **80** occurred at ca. 410-415 nm and 477 nm, respectively, due to the extended conjugation length of the pyrene chromophore with the four phenylethynylenic units. Interestingly, although the vibronic features of **79a-c** were more similar to those of **80** than to those of **76** (Figure 14), the spectra of **79** were less red-shifted than that of **80**, despite the presence of the two electron-donating *t*Bu groups in **79**. A reasonable explanation for these different shifts between **79** and **80** is their quite different conjugation pathway. For **79**, the four phenylacetylenic units are connected with the central pyrene moieties at the nearby 4-, 5-, 9-, and 10-positions to afford a short, cruciform, π-conjugated molecular structure, hence, short, cruciform π-conjugation occurs; for **80**, however, these four phenylacetylenic units are connected with pyrene rings at the more distant 1-, 3-, 6-, and 8-positions, resulting in a longer cruciform, π-conjugated structure. Hence, the conjugation length of **80** is larger than that of **79**, which leads to a larger red shift to ~ 500 nm. Upon excitation, a dilute solution of **79** and **80** in $CH_2Cl_2$ showed pure-blue and green emission (Figure 14) with a maximum band at 441 nm for **79a**, 448 nm for **79b**, 453 nm for **79c**, and 496 nm for **80**, respectively, which are systematically varied in agreement with

the electronic absorption spectra. High quantum yields of **79** in solution were found to in the range of 0.66-0.98.

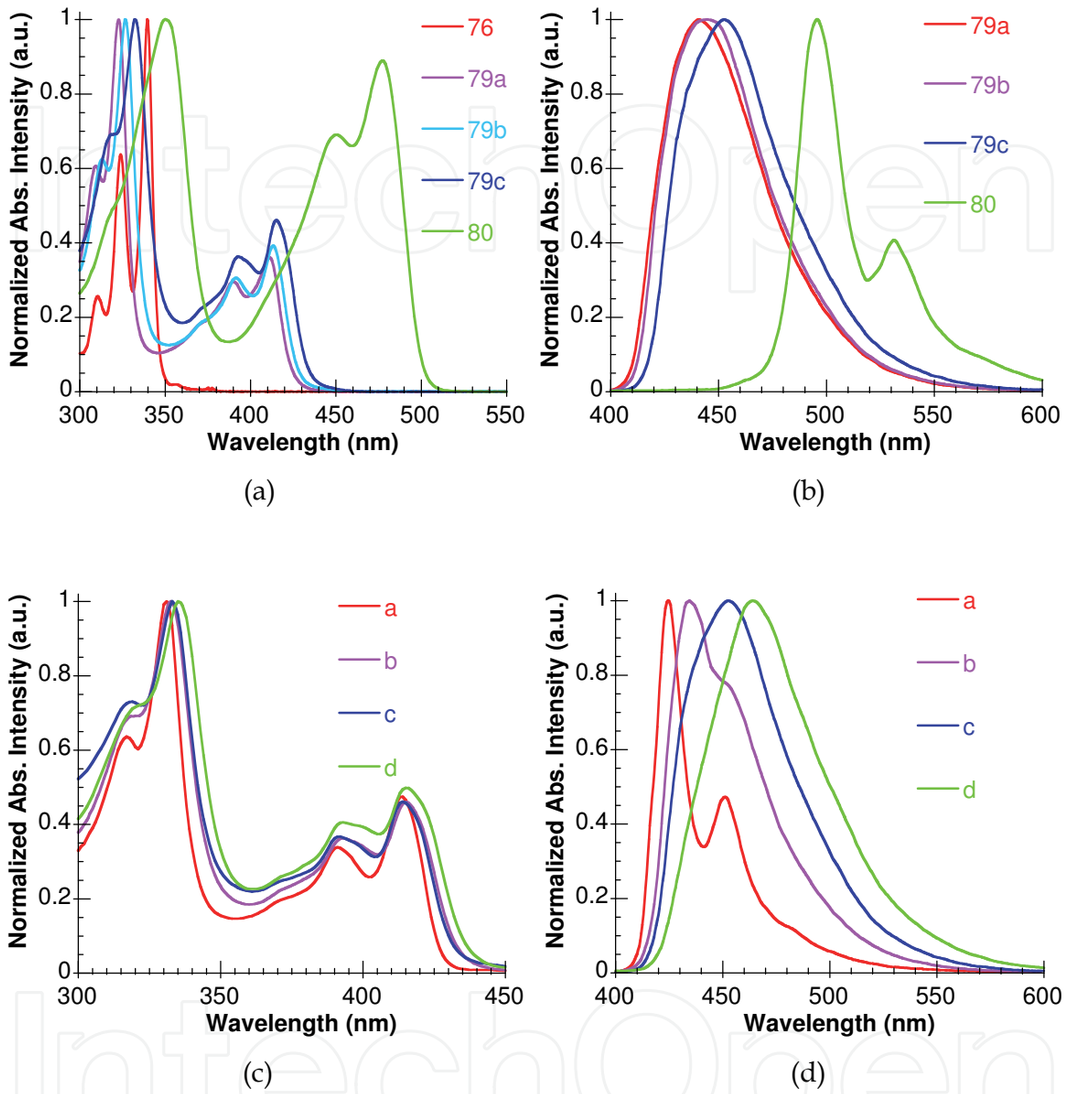


Fig. 14. Normalized absorption (A) and fluorescence emission spectra (B) of **79** and **80** recorded in $CH_2Cl_2$; down) Normalized absorption (C) and fluorescence emission spectra (D) of **79c** recorded in (a) cyclohexane, (b) THF, (c) $CH_2Cl_2$, and (d) DMF.

In order to obtain more insight into the photophysical properties of these new cruciform-shaped, conjugated pyrenes, both concentration dependence of the fluorescence and solvatochromic shifts of the absorption and emission spectra of **79c** are investigated, respectively. By increasing the concentration from $1.0 \times 10^{-8}$ M to $1.0 \times 10^{-4}$ M, the intensity of this emission band to gradually increase, only the monomer emission at 453 nm was observed. The result further indicate that the two sterically bulky *t*Bu groups at the 2- and 7-positions can prevent two molecules of **79** from getting close enough to result in excimer emission at high concentrations. For **79c**, a change of solvent from nonpolar cyclohexane to

polar DMF caused only a very slight, positive, batnochromic shift in the π-π* absorption band from 413 to 417 nm. However, in the case of the emission of **79c**, a substantial positive bathochromism with a maximum peak from 425 nm to 464 nm was observed fromcyclohexane to DMF (Figure 14). The results suggest that these new pyrenes **79** are more solvated in the excited state than in the ground state (Chew et al., 2007). Thus, these molecules emit very bright, pure-blue fluorescence and have good solubility in common organic solvents and high stability, which make them potential candidates as blue organic light-emitting materials for the fabrication of OLED devices, and further exploration into this area is underway.

## 7. Conclusions

In this Chapter, we have given an overview of the recent work on the synthesis and photophysical properties of pyrene-based light-emitting architectures and their application to molecular optoelectronic devices. We have demonstrated here some concrete examples that pyrene can be appropriately modified with electro- or photo-active chromosphores such as phenyl, phenylethynyl, fluorene, carbazole, and pyrene, and the resulting functional pyrenes can be successfully applied to the fabrication of EL devices. Thus, we expect that further research work on the functional pyrenes will promote a basic understanding of molecular design and optoelectronic properties, and their potential applications to molecular devices such as organic light-emitting diodes (OLEDs).

## 8. Acknowledgments

The authors wish to acknowledge financial support, respectively, from the CANON Company, the Royal Society of Chemistry and the Cooperative Research Program of "Network Joint Research Center for Materials and Devices (Institute for Materials Chemistry and Engineering, Kyushu University)". The authors wish to thank Dr. Yong-Jin Pu (Department of Organic Device Engineering, Yamagata University) for fruitful discussions.

## 9. References

Adachi, A.; Manhart, S. A.; Okita, K.; Kido, J.; Ohshita, J. & Kunai, A. (1997). *Synth. Met.*, 91, p. 333.

Adronov, A. & Frechet, J. M. J. (2000). *Chem. Commun.*, p. 1701.

An, B.-K.; Kwon, S.-K.; Jung, S.-J. & Park, S. Y. (2002). *J. Am. Chem. Soc.,* 124, p. 14410.

Anthony, J. E.; Heeney, M. & Ong, B. S. (2008). *MRS Bulletin,* 33, p. 698.

Anthopoulos, T. D.; Frampton, M. J.; Namdas, E. B.; Burn, P. L. & Samuel, I. D. W. (2004). *Adv. Mater.*, 16, p. 557.

Balaganesan, B.; Shen, W.-J. & Che, C.-H. (2003). *Tetrahedron Letters,* 44, p. 5747.

Balakrishnan, K.; Datar, A.; Oitker, R.; Chen, H.; Zuo, J. & Zang, L. (2005). *J. Am. Chem. Soc.,* 127, p. 10496.

Balakrishnan, K.; Datar, A.; Zhang, W.; Yang, X.; Naddo, T.; Huang, J.; Zuo, J.; Yen, M.; Moore, J. S. & Zang, L. (2006). *J. Am. Chem. Soc.*, 128, p. 6576.

Bandichhor, R.; Petrescu, A. D.; Vespa, A.; Kier, A. B.; Schroeder, F. & Burgess, K. (2006). *J. Am. Chem. Soc.*, 128, p. 10688.

Barboiu, M.; Prodi, L.; Montalti, M.; Zaccheroni, N.; Kyritsakas, N. & Lehn, J.-M. (2004). *Chem.-Eur. J.*, 10, p. 2953.

Bauer, R.; Liu, D. V.; Heyen, A.; Schryver, F. D.; Fryter, S. D.; & Mullen, K. (2007). *Macromolecules,* 40, p. 4753.

Becker, K.; Lupton, J. M.; Feldmann, J.; Setayesh, S.; Grimsdale, A. C.; & Mullen, K. (2006). *J. Am. Chem. Soc.,* 128, p. 680.

Bennistom, A. C.; Harriman, A.; Howell, S. L.; Sams, C. A. & Zhi, Y.-G. (2007). *Chem.-Eur. J.*, 13, p. 4665.

Benniston, A. C.; Harriman, A.; Lawrie, D. J.; Mayeux, A.; Rafferty, K.; & Russel, O. D. (2003). *Dalt. Trans.*, p. 4762.

Berlamn,I. B. (1970). *J. Phys. Chem.*, 74, p. 3085.

Bernhardt, S.; Kastler, M.; Enkelmann, V.; Baumgarten, M. & Mullen, K. (2006). *Chem.-Eur. J.*, 12, p. 6117.

Brabec, C. J.; Sariciftci, N. S. & Hummelen, J. C. (2001). *Adv. Funct. Mater.*, 11, p. 15.

Burroughes, J. H. Burroughes, J. H.; Bradley, D. D. C.; Brown, A. R.; Marks, R. N.; Mackay, K.; Friend, R. H.; Burnss, P. L. & Holmes, A. B. (1990). *Nature,* 347, p. 539.

Charles Li, X.-C.; Okamura, Y.; Ueno, K.; Tashiro, M.; & Surya Prakash, G. K. *US Patent* 6852429 2005.

Chen, B. J.; Lai, W. Y.; Gao, Z. Q.; Lee, C. S. & Gambling, W. A. (1999). *Appl. Phys. Lett.,* 75, p. 4010.

Chen, C. H. & Shi, J. (1998). *Coord. Chem. Rev.,* 171, p. 161.

Cheng, C.-H.; & Lin, C. –S. *US Patent* 0169921 2009.

Chen, S.; Xu, X.; Liu, Y.; Yu, G.; Sun, X.; Qiu, W.; Ma, Y. & Zhu, D. (2005). *Adv. Funct. Mater.*, 15, p. 1541.

Chew, S.; Wang, P.; Hong, Z.; Kwong, H. L.; Tang, J.; Sun, S.; Lee, C. S. & Lee, S.-T. (2007). *J. Lumin.,* 124, p. 221.

Chu, T.-Y. & Song, O.-K. (2007). *Appl. Phys. Lett.,* 90, p. 203512.

Clar, E. & Schmidt, W. (1976). *Tetrahedron,* 32, p. 2563.

Daub, J.; Beck, M.; Knorr, A. & Spreitzer, H. (1996). *Pure Appl. Chem.*, 68, p. 1399.

de Halleux, V.; Calbert, J.-P.; Brocorens, P.; Cornil, J.; Declercq, J.-P.; Bredas, J.-L. & Greets, Y. (2004). *Adv. Funct. Mater.*, 14, p. 649.

Ding, J. Q.; Gao, J.; Cheng, Y. X.; Xie, Z. Y.; Wang, L. X.; Ma, D. G.; Jing, X. B. & Wang, F. S. (2006). *Adv. Funct. Mater.*, 16, p. 575.

Duggal, A. R.; Heller, C. M.; Shiang, J. J.; Liu, J. & Lewis, L. N. (2007). *J. Displ. Tech.*, 3, p. 184.

Figueira-Duarte, T. M.; Del Rosso, P. G.; Trattnig, R.; Sax, S.; List, E. J. W. & Mullen, K. (2010). *Adv. Mater.*, 22, p. 990.

Figueira-Duarte, T. M.; Simon, S. C.; Wager, M.; Druzhinin, S. I.; Zachariasse, K. A. & Mullen, K. (2008). *Angew. Chem. Int. Ed.*, 47, p. 10175.

Fogel, Y.; Kastler, M.; Wang, Z.; Rienko, D.; Bodwell, G. J. & Mullen, K. (2007). *J. Am. Chem. Soc.*, 129, p. 11743.

Freeman, A. W.; Koene, S. C.; Malenfant, P. R. L.; Thompson, M. E. & Frechet, J. M. (2000). *J. Am. Chem. Soc.*, 122, p. 12385.

Fujimoto, K.; Shimizu, H.; Furusyo, M.; Akiyama, S.; Ishida, M.; Furukawa, U.; Yokoo, T. & Inouye, M. (2009). *Tetrahedron,* 65, p. 9357.

Gao, B.; Wang, M.; Cheng, Y.; Wang, L.; Jing, X. & Wang, F. (2008). *J. Am. Chem. Soc.*, 130, p. 8297.
Geffroy, B.; le Roy, P. & Prat C. (2006). *Poly. Inter.*, 55, p. 572.
Gingras, M.; Placide, V.; Raimundo, J.-M.; Bergamini, G.; Ceroni, P. & Balzani, V. (2008). *Chem.-Eur. J.*, 14, p. 10357.
Gong, L.-Z.; Hu, Q.-S. & Pu, L. (2001). *J. Org. Chem.*, 66, p. 2358.
Grimshaw, J. & Grimshaw, J. T. (1972). *J. Chem. Soc. Perkin Trans 1*, p. 1622.
Haley, M. M.; Tykwinski, R. R. (Eds), *Carbon-Rich Compounds: From Molecules to Materials*, Wiley-VCH: Weinheim, Germany, 2006.
Halim, M.; Pillow, J. N. G.; Samuel, I. D. W. & Burn, P. L. (1999). *Adv. Mater.*, 11, p. 371.
Han, J.; Jose, J.; Mei, E. & Burgess, K. (2007). *Angew. Chem. Int. Ed.*, 46, p. 1684.
Harth, E. M.; Hecht, S.; Helms, B.; Malmstrom, E. E.; Frechet, J. M. J. & Hawker, C. J. (2002). *J. Am. Chem. Soc.*, 124, p. 3926.
Hill, J. P.; Jin, W.; Kosawa, A.; Fukushima, T.; Ichihara, H.; Shimomura, T.; Ito, K.; Hashizime, T.; Ishii, N. & Aida, T. (2004). *Science,* 304, p. 1481.
Hoeben, F. J. M.; Jonkheijim, P.; Meijer, E. W. & Schenning, A. P. H. J. (2005). *Chem. Rev*, 105, p. 1491.
Hoger, S. *In Acetylene Chemistry*; Diederich, F.; Stang, P. J.; & Tykwinski, R. R. Eds.; Willey-VCH: Weinheim, Germany, 2005.
Hu, J.-Y.; Era, M.; Elsegood, M. R. J. & Yamato, T. (2010). *Eur. J. Org. Chem.*, 1, p. 72.
Hu, J.-Y.; Paudel, A. & Yamato, T. (2009). *J. Chem. Res.*, p. 109.
Hu, K.; Zhu, P. W.; Yu, Y.; Facchetti, A. & Marks, T. J. (2004). *J. Am. Chem. Soc.*, 126, p. 15974.
Hung, L. S. & Chen, C. H. (2002). *Mater. Sci. Engi. R. Rep.*, 39, p. 143.
Jacob, J.; Sax, S.; Plok, T.; List, E. J. W.; Grimsdale, A. C. & Mullen, K. (2004). *J. Am. Chem. Soc.*, 126, p. 6987.
Jiang, D. L.; & Aida, T. (1997*). Nature* (London) 388, p. 454.
Jiang, X.-Y.; Zhang, Z.-L.; Zheng, X.-Y.; Wu, Y.-Z. & Xu, S.-H. (2001). *Thin Solid Films*, 401, p. 251.
Jiao, G.-S.; Thoresen, L. H.; Kim, T. G.; Haaland, W. C.; Gao, F.; Topp, M. R.; Hochstrasser, R. M.; Metzker, M. L. & Burgess, K. (2006). *Chem.-Eur. J.,* 12, p. 7816.
Jia, W.-L.; Mccormick, T.; Liu, Q.-D.; Fukutani, H.; Moltala, M.; Wang, R.-Y.; Tao, Y. & Wang, S. (2004). *J. Mater. Chem.*, 14, p. 3344.
Jia, W. L.; Wang, R. Y.; Song, D. T.; Ball, S. J.; McLean, A. B. & Wang, S. N. (2005). *Chem.-Eur. J.*, 11, p. 832.
Joule, J. A. (1984). *Adv. Heterocycl. Chem.*, 35, p. 83.
Jurczok, M.; Plaza, P.; Rettig, W. & Martin, M. M. (2000). *Chem. Phys.*, 256, p. 137.
Kang, H.; Evrenenko, G.; Dutta, P.; Clays, K.; Song, K. & Marks, T. J. (2006). *J. Am. Chem. Soc.*, 128, p. 6194.
Kastler, M.; Pisula, W.; Wasser-fallen, D.; Pakula, T. & Mullen, K. (2004). *J. Am. Chem. Soc.*, 126, p. 5234.
Kawano, S.-I.; Yang, C.; Ribas, M.; Baluschev, S.; Baumgarten, M. & Mullen, K. (2008). *Macromolecules*, 41, p. 7933.
Kawase, T. (2007). *Synlett*, p. 2609.
Kido, J. & Lizumi, Y. (1997). *Chem. Lett.*, 26, p. 963.
Kim, H. M.; Lee, Y. O.; Lim, C. S.; Kim, J. S. & Cho, B. R. (2008). *J. Org. Chem.*, 73, p. 5127.

Kim, Y.-H.; Jeong, H.-C.; Kim, S.-H.; Yang, K. & Kwon, S.-K. (2005). *Adv. Funct. Mater.*, 15, p. 1799.

Kim, Y. H.; Shin, D. C.; Kim, S. H.; Ko, C. H;. Yu, H. S.; Chae, Y. S. & Kwon, S. K. (2001). *Adv. Mater.*, 13, p. 1690.

Kimura, M.; Shiba, T.; Yamazaki, M.; Hanabusa, K.; Shirai, H. & Kobayashi, N. (2001). *J. Am. Chem. Soc.*, 123, p. 5636.

Koene, B. E.; Loy, D. E. & Thompson, M. E. (1998). *Chem. Mater.*, 10, p. 2235.

Kraft, A.; Grimsdale, A. & Holmes, A. B. (1998). *Angew. Chem. Int. Ed.*, 37, p. 402.

Krebs, F. C. (2009). *Solar Energy Materials and Solar Cells,* 93, p. 394.

Kulkarni, A. P.; Tonzola, C. J.; Babel, A. & Jenekhe, S. A. (2004). *Chem. Mater.*, 16, p. 4556.

Kuwabara, Y.; Ogawa, H.; Inada, H.; Noma, N. & Shirota, Y. (1994). *Adv. Mater.*, 6, p. 677.

Kwok, C. C. & Wong, M. S. (2001). *Macromolecules,* 34, p. 6821.

Law, M. Goldberger, J.; & Yang, P. D. (2004). *Ann. Rev. Mater. Res.*, 34, p. 83.

Lee, S. H.; Nakamura, T. & Tsutui, T. (2001). *Org. Lett.*, 3, p. 2005.

Lehn, J.-M. *Supramolecular Chemistry-Concepts and Perspectives*; VCH: Weiheim, Germany, 1995.

Liao, Y.-L.; Lin, C.-Y.; Wong, K.-T.; Hou, T.-H. & Hung, W.-Y. (2007). *Org. Lett.*, 10, p. 4511.

Liu, D. J.; De Feyter, S.; Cotlet, M.; Stefan, A.; Wiesler, U. M.; Herrmann, A.; Grebel-Koehler, D.; Qu, J. Q.; Mullen, K. & De Schryver, F. C. (2003). *Macromolecules,* 36, p. 5918.

Liu, F.; Tang, C.; Chen, Q.-Q.; Li, S.-Z.; Wu, H.-B.; Xie, L.-H.; Peng, B.; Wei, W.; Cao, Y. & Huang, W. (2009). *Organic Electronics,* 10, p. 256.

Loo, Y. L. & McCulloch, I. (2008). *MRS Bull.*, 33, p. 653.

Lo, S.-C.; Male, N. A.; Markham, J. P. J.; Magennis, S. W.; Burn, P. L.; Salata, O. V. & Samuel. I. D. W. (2002). *Adv. Mater.*, 14, p. 975.

Lo, S.-C.; Namdas, E. B.; Burn, P. L. & Samuel, I. D. W. (2003). *Macromolecules,* 36, p. 9721.

Loudet, A.; Bandichhor, R.; Wu, L. & Burgess, K. (2008). *Tetrahedron,* 64, p. 3642.

Lupton, J. M.; Samuel, I. D. W.; Beavington, R.; Frampton, M. J.; Burn, P. L. & Bassler, H. (2001). *Phys. Rev. B,* 63, p. 155206.

Maeda, H.; Maeda, T.; Mizuno, K.; Fujimoto, K.; Shimizu, H. & Inouye, M. (2006). *Chem.-Eur. J.,* 12, p. 824.

Manhart, S. A.; Adachi, A.; Sakamaki, K.; Okita, K.; Ohshita, J.; Ohno, T.; Hamaguchi, T.; Kunai, A. & Kido, J. (1999). *J.Organomet. Chem.*, 592, p. 52.

Markham, J. P. J.; Samuel, I. D. W.; Lo, S.-C.; Burn, P. L.; Weiter, M. & Bassler, H. (2004). *J. Appl. Phys.*, 95, p. 438.

Marsden, J. A.; Miller, J. J.; Shirtcliff, L. D. & Haley, M. M. (2005). *J. Am. Chem. Soc.*, 127, p. 2464.

Martin, R. B.; Qu, L.; Harruff, B. A.; Bunker, C. E.; Gord, J. R.; Allard, L. F. & Sun, Y.-P. (2004). *J. Phys. Chem. B*, 108, p. 11447.

McGehee, M. D. & Heeger, A. J. (2000). *Adv. Mater.,* 12, p. 1655.

Meijere, A. de. (Ed.), *Topics in Current Chemistry, Carbon Rich Compounds,* I, Spinger: Berlin, Germany, 196 1998.

Melhuish, W. H. (1961). *J. Phys. Chem.,* 65, p. 229.

Melinger, J. S.; Pan, Y.; Kleiman, V. D.; Peng, Z.; Davis, B. L.; McMorrow, D. & Lu, M. (2002). *J. Am. Chem. Soc.*, 124, p. 12002.

Miao, Q.; Chi, X. L.; Xiao, S. X.; Zeis, R.; Lefenfeld, M.; Siegrist, T.; Steigerwald, M. L. & Nuckolls, C. (2006). *J. Am. Chem. Soc.*, 128, p. 1340.

Mikroyannidis, J. A.; Fenenko, L. & Adachi, C. (2006). *J. Phys. Chem. B,* 110, p. 20317.

Mikroyannidis, J. A.; Persephonis, P. G. & Giannetas, V. G. (2005). *Synth. Met.,* 148, p. 293.

Modrakowski, C.; Flores, S. C.; Beinhoff, M. & Schluter, A. D. (2001). *Synthesis*, p. 2143.

Moorthy, J. N.; Natarajin, P.; Venkatakrishnan, P.; Huang, D.-F. & Chow, T. J. (2007). *Org. Lett.*, 9, p. 5215.

Mullen, K.; & Wegner, G. Eds: *Electronic Materials: The Oligomer Approach*, Wiley-VCH: Weinheim, Germany, 1998.

Mullen, K.; Scherf, U. Eds: *Organic Light Emitting Devices: Synthesis Properties and Applications* Wiley-VCH: Weiheim, Germany, 2006.

Naraso; Nishida, J.-I.; Ando, S.; Yamaguchi, J.; Itaka, K.; Koinuma, H.; Tada, H.; Tokito, S. & Yamashita, Y. (2005). *J. Am. Chem. Soc.*, 127, p. 10142.

Newkome, G. R.; Moorefield, C. N.; & Vogtle, F. *Dendritic Molecules: Comcepts, Synthesis, and Perspectives*, Wiley-VCH, Weinheim, Germany 1996.

O'Brien, D. F.; Burrows, P. E.; Forrest, S. R.; Koene, B. E.; Loy, D. E. & Thompson, M. E. (1998). *Adv. Mater.,* 10, p. 1108.

Oh, H.-Y.; Lee, C.-H. & Lee, S.-H. (2009). *Organic Electronics,* 10, p. 163.

Oh, J.-W.; Lee, Y. O.; Kim, T. H.; Ko, K. C.; Lee, J. Y.; Kim, H. & Kim, J. S. (2009). *Angew. Chem. Int. Ed.*, 48, p. 2522.

Ohshita, J.; Yoshimoto, K.; Tada, Y.; Harima, Y.; Kunai, A.; Kunugi, Y. & Yamashita, K. (2003*). J. Organomet. Chem.*, 678, p. 33.

Otsubo, T.; Aso, Y. & Takamiya, K. (2002). *J. Mater. Chem.,* 12, p. 2565.

Oyamada, T.; Uchiuzou, H.; Akiyama, S.; Oku, Y.; Shimoji, N.; Matsushige, K.; Sasaba, H. & Adachi, C. (2005). *J. Appl. Phys.*, 98, p. 074506.

Pogantsch; Wenzl, F. P.; List, E. J. W.; Leising, G.; Grimsdale, A. C.; & Mullen, K. (2002). *Adv. Mater.*, 14, p. 1061.

Pu, Y.-J.; Higashidate, M.; Nakayama, K. & Kido, J. (2008). *J. Mater. Chem.*, 18, p. 4183.

Qu, L. & Shi, G. (2004). *Chem. Commun.,* p. 2800.

Rathore, R.; Burns, C. L. & Abdelwahed, S. A. (2004). *Org. Lett.*, 6, p. 1689.

Rathore, R.; Burns, C. L. & Deselnicu, M. I. (2001). *Org. Lett.*, 3, p. 2887.

Rausch, D. & Lambert, C. (2006). *Org. Lett.*, 8, p. 5037.

Raytchev, M.; Pandurski, E.; Buchvarov, I.; Modrakowski, C. & Fiebig, T. (2003). *J. Phys. Chem. A*, 107, p. 4592.

Rivera, E.; Belletete, M.; Zhu, X. X.; Durocher, G. & Giasson, R. (2002). *Polymer,* 43, p. 5059.

Rosenfeldt, S.; Dingenouts, N.; Potschke, D.; Ballauff, M.; Berresheim, A. J.; Mullen, K.; & Linder, P. (2003). *Angew. Chem.*, 115, p. 111; (2004). *Angew. Chem. Int. Ed.*, 43, p. 109.

Sagara, Y.; Mutai, T.; Yoshikawa, I. & Araki, K. (2007). *J. Am. Chem. Soc.*, 129, p. 1520.

Sakamoto, Y.; Suzuki, T.; Miura, A.; Fujikawa, H.; Tokito, S. & Taga, Y. (2000). *J. Am. Chem. Soc.*, 122, p. 1832.

Salbeck, J.; Weissortel, F.; Yu, N.; Baner, J. & Bestgen, H. (1997). *Synth. Met.*, 91, p. 209.

Seminario, J. M. (2005). *Nature Materials,* 4, p. 111.

Shibano,Y.; Umeyama, T.; Matano, Y. & Imahori, H. (2007). *Org. Lett.,* 10, p. 1971.

Shih, H. T.; Lin, C.-H.; Shih, H.-H.; & Cheng, C.-H. (2002). *Adv. Mater.,* 14, p. 1409.

Shi, J.; Wang, C. W.; & Chen, C. H. *US Patent* 5646948, 1997.

Shtein, M.; Peumans, P.; Benziger, J. B. & Forrest, S. R. (2004). *Adv. Mater.*, 16, p. 1615.
Sienkowska, M. J.; Farrar, J. M.; Zhang, F.; Kusuma, S.; Heiney, P. A. & Kaszynski, P. (2007). *J. Mater. Chem.,* 17, p. 1399.
Shimizu, H.; Fujimoto, K.; Furusyo, M.; Maeda, H.; Nanai, Y.; Mizuno, K. & Inouye, M. (2007). *J. Org. Chem.*, 72, p. 1530.
Sirringhaus, H. & Ando, M. (2008). *MRS Bull.,* 33, p. 676.
So, F.; Kido, J. & Burrows, P. L. (2008). *MRS Bull.,* 33, p. 663.
Sonar, P.; Soh, M. S.; Cheng, Y. H.; Henssler, J. T. & Sellinger, A. (2010). *Org. Lett.*, 12, p. 3292.
Son, S.; Dodabalapur, A.; Lovinger, A. J. & Galvin, M. E. (1995). *Science*, 269, p. 376.
Strohriegl, P.; & Grazulevicius, J. V. (2002). *Adv. Mater.*, 14, p. 1439.
Strauss, J. & Daub, J. (2002). *Org. Lett.*, 4, p. 683.
Sun, D. L.; Rosokha, S. V. & Kochi, J. K. (2005). *Angew. Chem. Int. Ed.,* 44, p. 5133.
Swager, T. M. *In acetylene chemsity*; Diederich, F.; Stang, P. J.; & Tykwinski, R. R.; Eds; Willey-VCH: Weinheim, Germany, 2005.
Swager, T. M. & Zheng, J. (2005). *Advances in Polymer Science,* 177, p. 151.
Tang, C.; Liu, F.; Xia, Y.-J.; Lin, J.; Xie, L.-H.; Wei, A.; Li, S.-B.; Fan, Q.-L. & Huang, W. (2006). *J. Mater. Chem.*, 16, p. 4074.
Tang, C.; Liu, F.; Xia, Y.-J.; Lin, J.; Xie, L.-H.; Zhong, G.-Y.; Fan, Q.-L. & Huang, W. (2006). *Organic Electronics*, 7, p. 155.
Tang, C. W. & VanSlyke, S. A. (1987). *Appl. Phys. Lett.,* 51, p. 913.
Tao, S. L.; Hong, Z. R.; Peng, Z. K.; Ju, W. G.; Zhang, X. H.; Wang, P. H.; Wu, S. K. & Lee, S. T. (2004). *Chem. Phys. Lett.*, 397, p. 1.
Tao, S. L.; Peng, Z. K.; Zhang, X. H.; Wang, P. F.; Lee, C.-S. & Lee, S.-T. (2005). *Adv. Funct. Mater.*, 15, p. 1716.
Tao, S. L.; Zhou, Y.; Lee, C.-S.; Zhang, X.-H. & Lee, S.-T. (2010). *Chem. Mater.*, 22, p. 2138.
Thomas, K. R. J.; Velusamy, M.; Lin, J. T.; Chuen, C. H. & Tao, Y. T. (2005). *J. Mater. Chem.*, 15, p. 4453.
Thomas, K. R.; Lin, J T.; Tao, Y.-T.; & Ko, C.-W. (2000). *Adv. Mater.*, 12, p. 1949.
Thomas, K. R.; Lin, J T.; Tao, Y.-T. & Ko, C.-W. (2001). *J. Am. Chem. Soc.,* 23, p. 9404.
Tokito, S.; Tanaka, H.; Koda, N.; Okada, A. & Tago, Y. (1997). *Macromol. Symp.*, 125, p. 181.
Tonzola, C. J.; Alam, M. M.; Kaminsky, W. & Jenekhe, S. A. (2003). *J. Am. Chem. Soc.*, 125, p. 13548.
Tsumura, A.; Koezuka, K. & Ando, T. (1986). *Appl. Phys. Lett.*, 49, p. 1210.
Tu, G.; Zhou, Q.; Cheng, Y.; Wang, L.; Ma, D.; Jing, X. & Wang, F. (2004). *Appl. Phys. Lett.,* 85, p. 2172.
Uchida, M.; Izumizawa, T.; Nakano, T.; Yamaguchi, S.; Tamao, K. & Furukawa, K. (2001). *Chem. Mater.,* 13, p. 2680.
VandenBout, D. A.; Yip, W. T.; Hu, D. H.; Fu, D. K.; Swager, T. M. & Barbara, P. F. (1997). *Science*, 277, p. 1074.
Van der Auweraer, M. & De Schryer, F. C. (2004). *Nature Materials,* 3, p. 507.
Venkataramana, G. & Sankararaman, S. (2005). *Eur. J. Org. Chem.,* 19, p. 4162.
Venkataramana, G. & Sankararaman, S. (2006). *Org. Lett.*, 8, p. 2739.
Vollmann, H.; Becker, M.; & Correll, H. S. (1937). *Justus Liebigs Ann. Chem.*, 1, p. 531.

Wang, L.; Jiang, Y.; Luo, J.; Zhou, Y.; Zhou, J.; Wang, J.; Pei, J. & Cao, Y. (2009). *Adv. Mater.*, 21, p. 4854.
Wang, P. W.; Liu, Y. J.; Devadoss, C.; Bharathi, P. & Moore, J. S. (1996). *Adv. Mater.*, 8, p. 237.
Weinfurtner, K.-H.; Fujikawa, H.; Tokito, S. & Taga, Y. (2000). *Appl. Phys. Lett.*, 76, p. 2502.
Wilson, J. N. & Bunz, U. H. F. (2005). *J. Am. Chem. Soc.*, 127, p. 4124.
Wind, M.; Wiesler, U. M.; Saalwachter, K.; Mullen, K.; & Spiess, H. W. (2001). *Adv. Mater.*, 13, p. 752.
Wong, K. T.; Chien, Y. Y.; Chen, R. T.; Wang, C. F.; Lin, Y. T.; Chiang, H. H.; Hsieh, P. Y.; Wu, C. C.; Chou, C. H.; Su, Y. O.; Lee, G. P. & Peng, S. M. (2002). *J. Am. Chem. Soc.*, 124, p. 11576.
Wu, C.-C., Chen, C.-W.; Lin, C.-L. & Yang, C.-J. (2005). *J .Displ. Tech.*, 1, p. 248.
Wu, J.; Pisula, W. & Mullen, K. (2007*). Chem. Rev.*, 107, p. 718.
Wu, K.-C.; Ku, P.-J.; Lin, C.-S.; Shih, H.-T.; Wu, F.-I.; Huang, M.-J.; Lin, J.-J.; Chen, I.-C.; & Cheng, C.-H. (2008). *Adv. Funct. Mater.*, 18, p. 67.
Xie, W.; Hou, J. & Liu, S. (2003). *Semicond. Sci. Tech.,* 18, p. 142.
Xing, Y.-J.; Xu, X.-J.; Zhang, P.; Tian, W.–J.; Yu, G.; Lu, P.; Liu, Y.-Q. & Zhu, D.-B. (2005). *Chem. Phys. Lett.,* 408, p. 169.
Xu, M.-H.; Lin, J.; Hu, Q.-S. & Pu, L. (2002). *J. Am. Chem. Soc.*, 124, p. 14239.
Xu, Z. & Moore, J. S. (1993). *Angew. Chem. Int. Ed. Engl.*, 32, p. 1354.
Yamana, K.; Iwai, T.; Ohtani, Y.; Sato, S.; Namakura, M. & Nakano, H. (2002). *Bioconjugate Chem.*, 13, p. 1266.
Yamamoto, T. (2003). *Synlett*, 4, p. 425.
Yamashita, E. & Maeda, K. (2008). *Macromolecules,* 41, p. 3.
Yamato, T.; Fujimoto, M.; Miyazawa, A. & Matsuo, K. (1997). *J. Chem. Soc. Perkin Trans 1*, p. 1201.
Yamato, T.; Miyazawa, A. & Tashiro, M. (1993). *J. Chem. Soc. Perkin Trans 1*, p. 3127.
Yang, C.-H.; Guo, T.-F. & Sun, I.-W. (2007). *J. Lumine.*, 124, p. 93.
Yu, W.-L.; Pei, J.; Huang, W. & Heeger, A. J. (2000). *Adv. Mater.*, 12, p. 828.
Zen, A.; Bilge, A.; Galbrecht, F.; Alle, R.; Meerholz, K.; Grenzer, J.; Neher, D.; Scherf, U. & Farrell, T. (2006). *J. Am. Chem. Soc.,* 128, p. 3914.
Zhang, H.-J.; Wang, Y.; Shao, K.-Z.; Liu, Y.-Q.; Chen, S.-Y.; Qiu, W.-F.; Sun, X.-B.; Qi, T.; Ma, Y.-Q.; Yu, G.; Su, Z-.M. & Zhu, D.-B. (2006). *Chem. Commun.*, 2, p. 755.
Zhang, M.; Xue, S.; Dong, S.; Wang, Q.; Fei, T.; Gu, C. & Ma, Y. (2010). *Chem. Commun.*, 46, p. 3923.
Zhao, Z. J.; Li, J.-H.; Chen, X. P.; Lu, P. & Yang, Y. (2008). *Org. Lett.,* 10, p. 3041.
Zhao, Z. J.; Li, J.-H.; Chen, X. P.; Wang, X. M.; Lu, P. & Yang, Y. (2009). *J. Org. Chem.*, 74, p. 383.
Zhao, Z. J.; Xu, X. J.; Jiang, Z. T.; Lu, P.; Yu, G. & Liu, Y. Q. (2007). *J. Org. Chem.*, 72, p. 8345.
Zhao, Z. J.; Xu, X. J.; Wang, F.; Yu, G.; Lu, P.; Liu, Y. & Zhu, D. (2006). *Synth. Met.*, 156, p. 209.

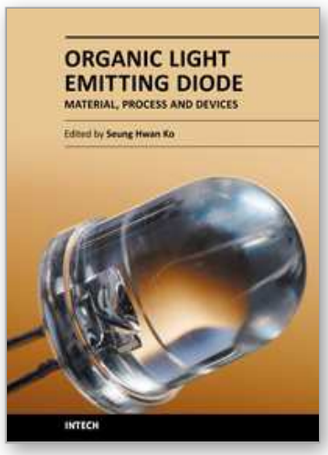


**Organic Light Emitting Diode - Material, Process and Devices**

Edited by Prof. Seung Hwan Ko

ISBN 978-953-307-273-9
Hard cover, 322 pages
**Publisher** InTech
**Published online** 27, July, 2011
**Published in print edition** July, 2011

This book contains a collection of latest research developments on Organic light emitting diodes (OLED). It is a promising new research area that has received a lot of attention in recent years. Here you will find interesting reports on cutting-edge science and technology related to materials, fabrication processes, and real device applications of OLEDs. I hope that the book will lead to systematization of OLED study, creation of new research field and further promotion of OLED technology for the bright future of our society.



**InTech Europe**
University Campus STeP Ri
Slavka Krautzeka 83/A
51000 Rijeka, Croatia
Phone: +385 (51) 770 447
Fax: +385 (51) 686 166
www.intechopen.com

**InTech China**
Unit 405, Office Block, Hotel Equatorial Shanghai
No.65, Yan An Road (West), Shanghai, 200040, China
中国上海市延安西路65号上海国际贵都大饭店办公楼405单元
Phone: +86-21-62489820
Fax: +86-21-62489821

IntechOpen